Chapitre 2
Methods and techniques

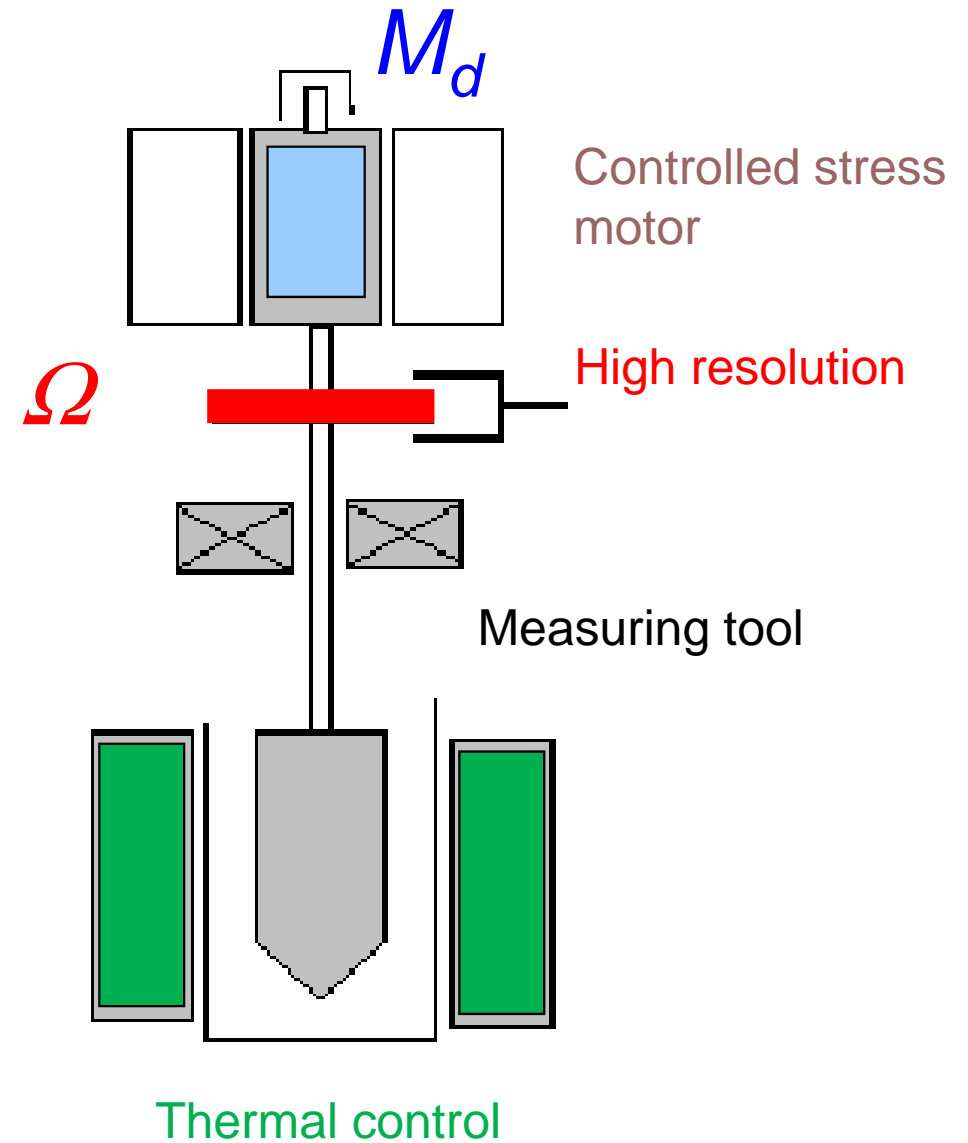# 2.1 Macroscopic rheology

Controlled strain/rate rheometer

ARES 2000

M (torque)

Transducer

$$\sigma = A \cdot M$$

Measuring tool

Thermal control

Motor
Air bearing

$$\dot{\gamma} = C \cdot \Omega$$
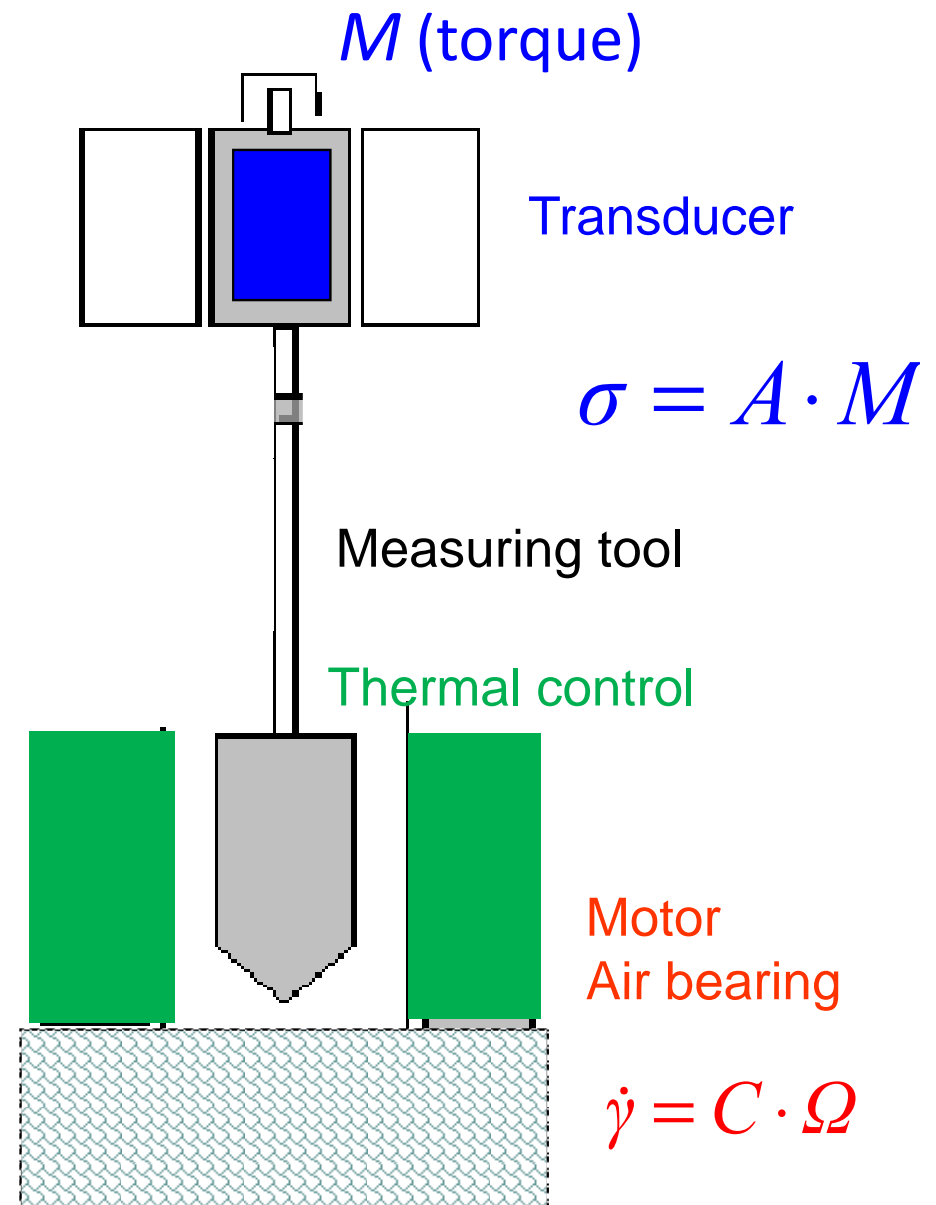
Controlled stress rheometer

M_d

Controlled stress motor

Ω

High resolution

Measuring tool

Thermal control

Measuring tools

Concentric Cylinders — Very Low to Medium Viscosity

Cone and Plate — Very Low to High Viscosity

Parallel Plate — Very Low Viscosity to Soft Solids

Torsion Rectangular — Very Soft to Very Rigid Solids
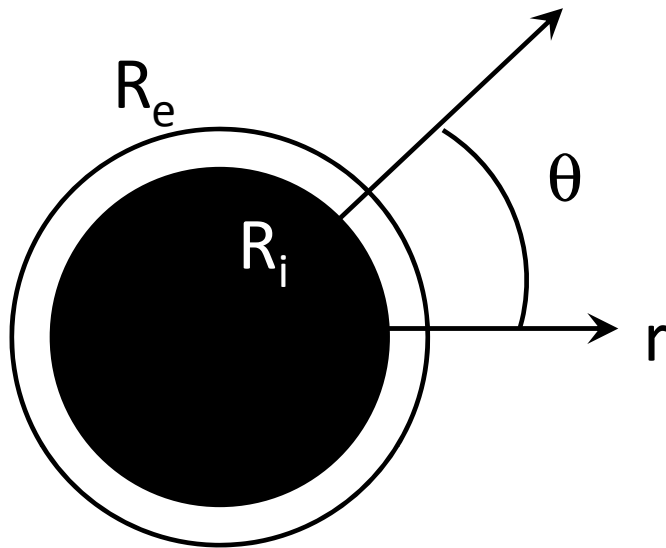
water ⟶ steel

5

Couette geometry

Ω

L

R_0

R_i
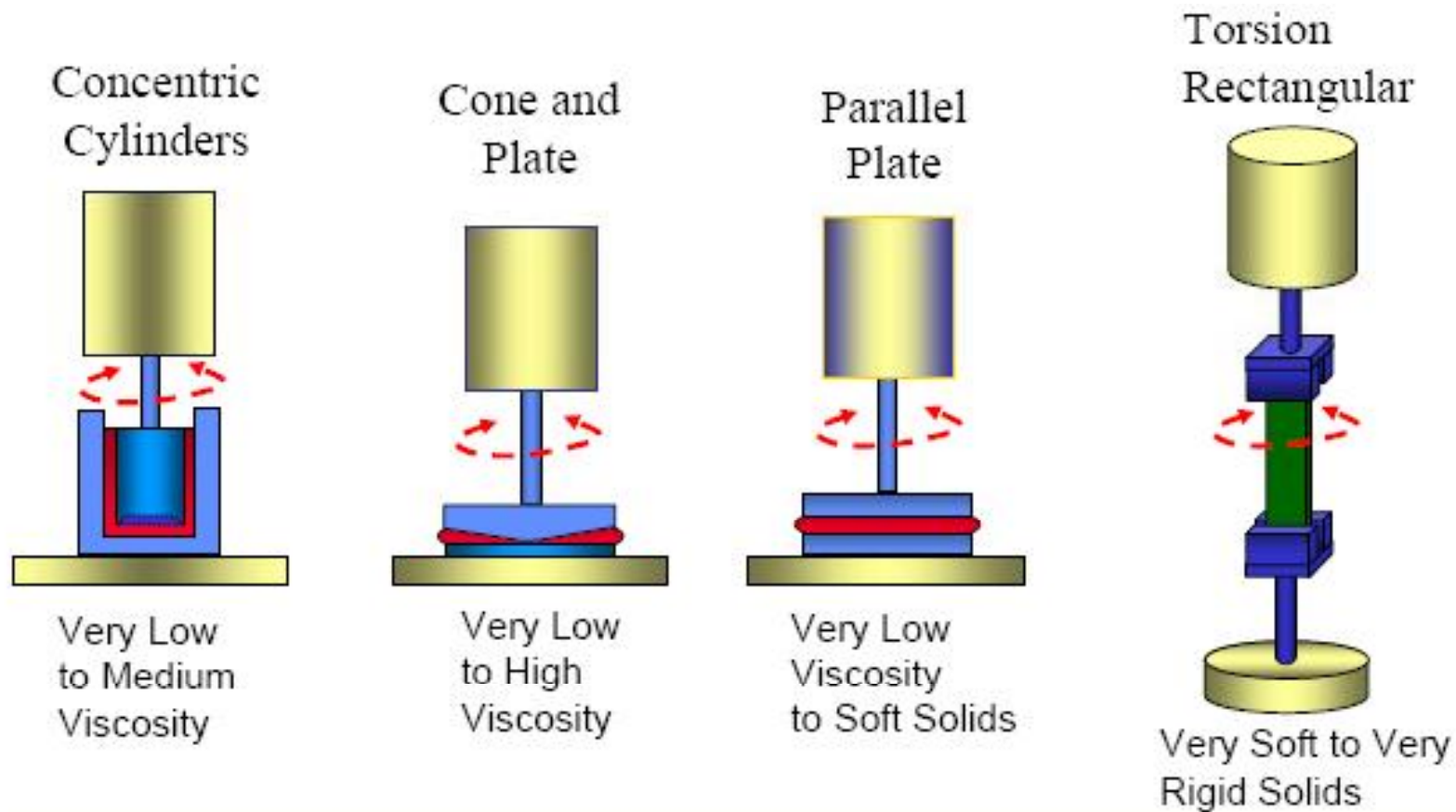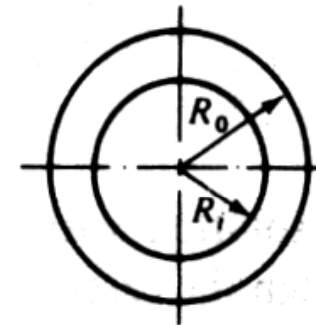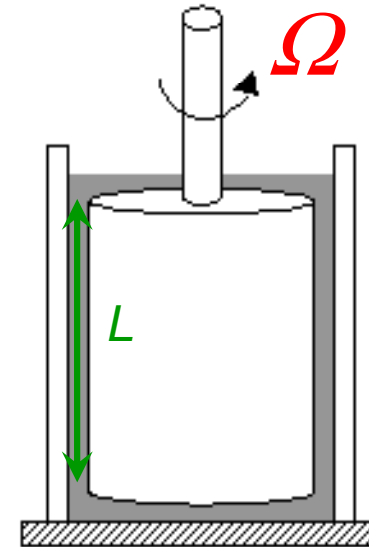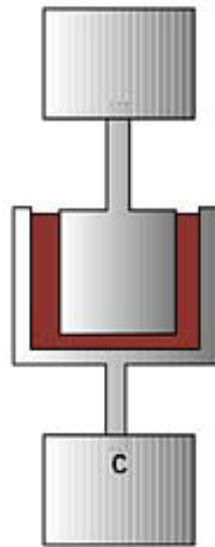
Low viscosities (solutions): $\eta_0 < 1$ Pa.s

High shear rates

Not suited for viscous liquids or melts

Flow in a cylindrical Couette

R_e

R_i

θ

r

Laminar flow

$V_\theta = r\Omega$

No gravity

Symmetry $/\theta$: $\partial/\partial\theta = 0$

$\mathbf{T} = -p\mathbf{I} + \sigma$

Navier Stokes equations (cylindrical coordinates)

$$-\rho\frac{V_\theta^2}{r} = \frac{1}{r}\frac{\partial(rT_{rr})}{\partial r} - \frac{T_{\theta\theta}}{r} = \frac{\partial(\sigma_{rr})}{\partial r} - \frac{\sigma_{\theta\theta} - \sigma_{rr}}{r}$$

$$\frac{\partial(r^2\sigma_{r\theta})}{\partial r} = 0$$

$$\sigma_{r\theta} = \frac{\sigma_i R_i^2}{r^2}$$

$$-\frac{\partial p}{\partial z} + \rho g = 0$$

Hydrostatic pressure

Relation between torque and stress

The shear stress varies through the gap between the cylinders

At the inner cylinder:

$$\frac{M_i}{R_i} = \sigma_{r\theta}(R_i)2\pi R_i L$$

$$\sigma_{r\theta}(R_i) = \frac{M_i}{2\pi R_i^2 L}$$

M_i: torque applied on, or measured at, the inner cylinder

Strain and strain rate

For small gaps, $R_i / R_e > 0.99$, we can neglect the curvature (~parallel plates):

$$\overline{\gamma} = \frac{\Delta x(r)}{\Delta r} = \frac{\theta \overline{R}}{R_e - R_i} \text{ with } \overline{R} = \frac{R_e + R_i}{2}$$

Similarly for the shear rate:

$$\dot{\overline{\gamma}} = \frac{\Delta v(r)}{\Delta r} = \frac{\Omega_i \overline{R}}{R_e - R_i} \text{ avec } \overline{R} = \frac{R_e + R_i}{2}$$

General expressions exist for large gaps:

$$\dot{\gamma}_i = 2\Omega_i \frac{d \, Ln(\Omega_i)}{d \, Ln(M_i)}$$

Normal stresses

Normal stresses are: $T_{\theta\theta}$ et T_{rr}

The first normal stress difference is:

$$N_1 = T_{\theta\theta} - T_{rr} = \sigma_{\theta\theta} - \sigma_{rr}$$

In the absence of inertia:

$$0 = \frac{\partial(\sigma_{rr})}{\partial r} - \frac{\sigma_{\theta\theta} - \sigma_{rr}}{r}$$

$$N_1 = r\frac{\partial(\sigma_{rr})}{\partial r}$$

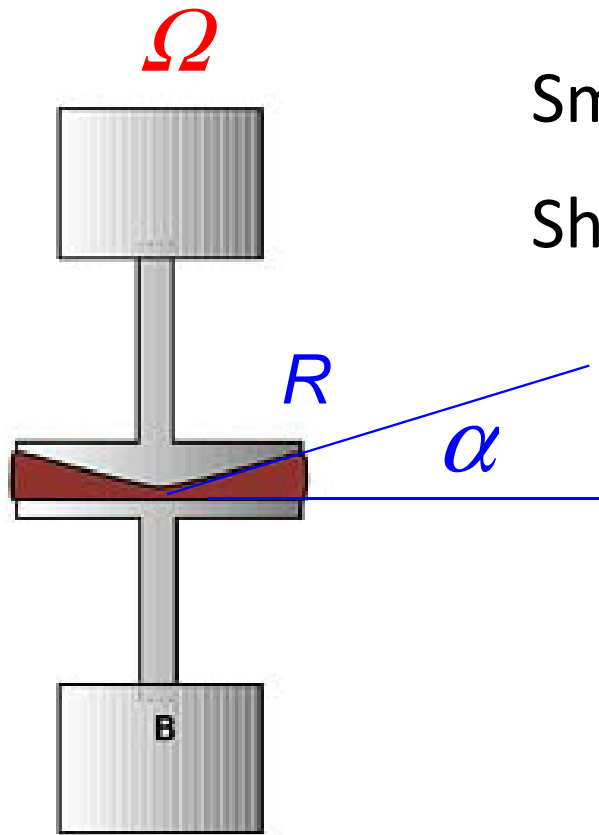$$N_1 = \left[\sigma_{rr}(R_i) - \sigma_{rr}(R_e)\right]\frac{\overline{R}}{R_0 - R_i}$$

Difficult to measure
Pressure sensors located
on the cylinders
Small pressures

Cone and plate geometry

The shear rate is constant inside the gap

Small or moderate viscosities

Shear rate: 10^{-3}-10^{2} s^{-1}

$$\sigma = \frac{3M}{2\pi R^3}$$

$$\dot{\gamma} = \frac{\Omega}{\alpha}$$

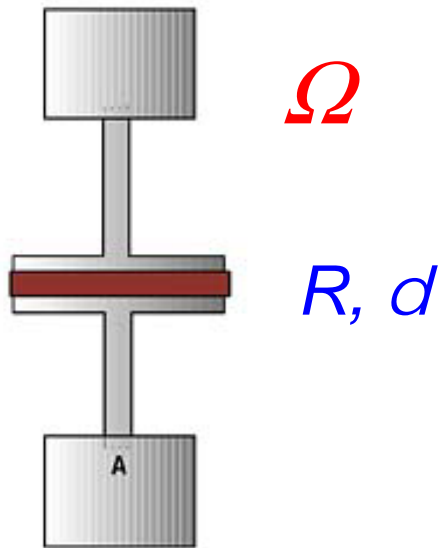$$N_1 = \frac{2F_n}{\pi R^2}$$

Ω

R

α

B

Parallel plate geometry

Loading is easy

Well adapted to polymer melts, pastes, or highly viscous liquids

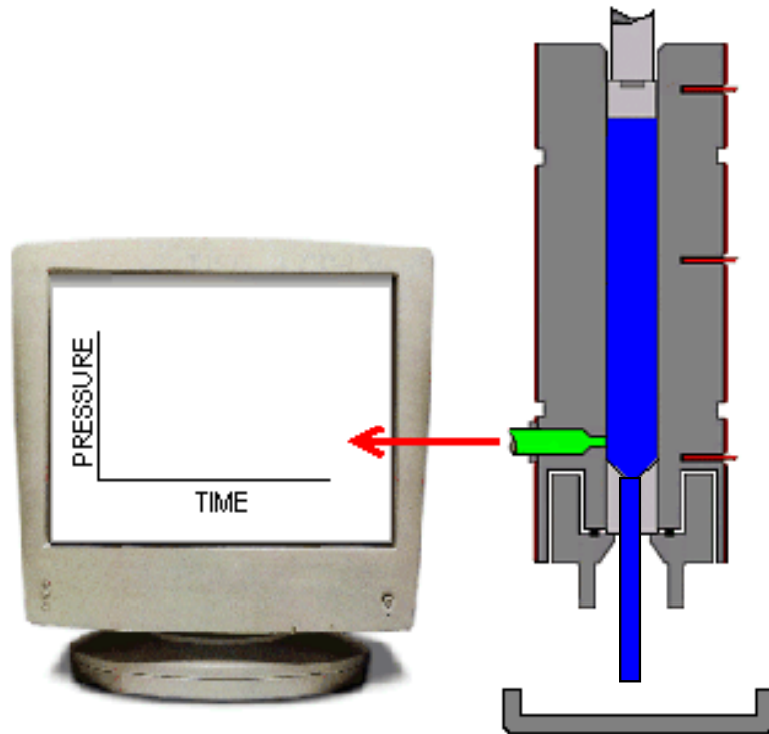γ, $\dot{\gamma}$ and σ vary with r, measurements are given at $r=R$

Ω

R, d

$$\dot{\gamma}_R = \frac{R\Omega}{d}$$

$$\sigma_R = \frac{3M}{2\pi R^3}\left(1 + \frac{1}{3}\frac{d\ln M}{d\ln\dot{\gamma}_R}\right)$$

$$(N_1 - N_2)_R = \frac{F_n}{\pi R^2}\left(2 + \frac{d\ln F_n}{d\ln\dot{\gamma}_R}\right)$$

Capillary rheometer

The material (paste, polymer melt) is pushed through a capillary
The applied stress depends on the properties of the material

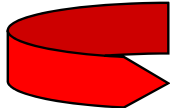$$\dot{\gamma}_a = \frac{4Q}{\pi R^3}, \sigma_a = \frac{R\Delta P}{2L}$$

Entrance: Bagley corrections
Power law fluids: Rabinovitch correction

Domains of applications: highly viscous /elastic materials and high shear rates (100/1000 s^{-1})

Rheological protocols

σ (stress) γ (strain)

Small deformation   Large deformation
Linear response   Non linear response
Equilibrium structure   Out of equilibrium structure

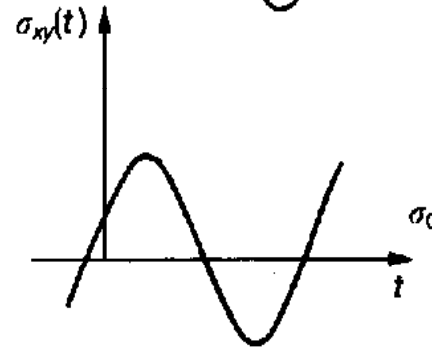$$\dot{\gamma}\tau \ll 1$$ $$\dot{\gamma}\tau \gg 1$$

Mechanical spectroscopy (small deformations)
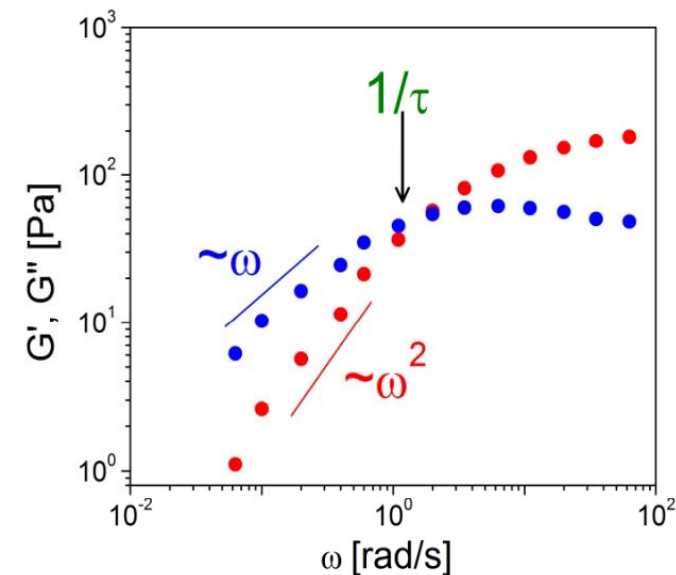
Excitation
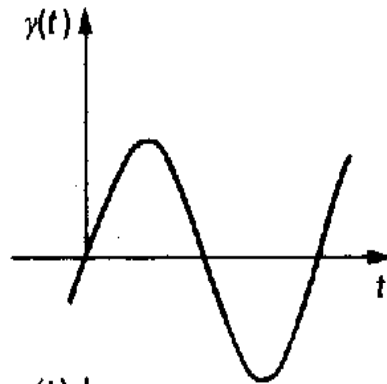
$$\gamma(t) = \gamma_0 \cos(\omega t)$$

Response

In-phase component: G'(ω)
Elasticity – storage modulus

Out of phase component: G"(ω)
Dissipation – loss modulus

Example: entangled polymer solution

Strengths and drawbacks

- "easy" to implement
- a huge theoretical and experimental background is available
- the dynamics reflects/is associated with the equilibrium structure

- Large amounts of products are necessary (>1 ml)
- In-vivo measurements are not possible (biology)
- The low deformation limit may be difficult to acheive
- The accessible frequency window is narrow ($10^{-2} < \omega < 10^{2}$ rad/s)
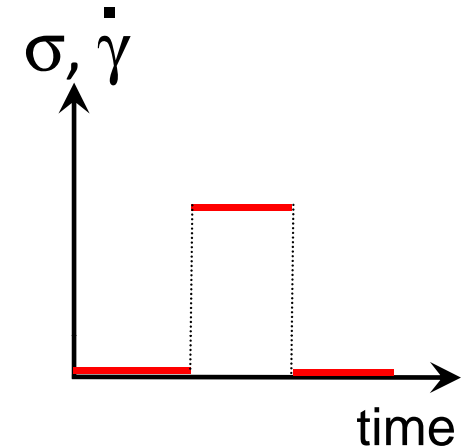
Non-linear rheology

Many experimental tests can be implemented

$\sigma, \dot{\gamma}, \gamma$

time

σ

time

$\sigma, \dot{\gamma}$

time
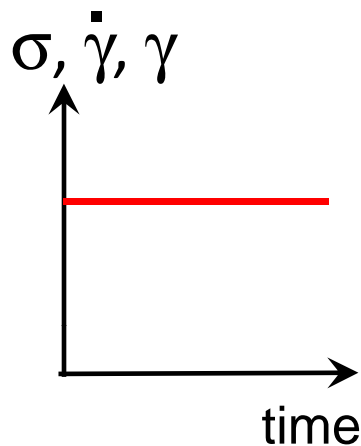
Creep (σ)
Steady shear ($\dot{\gamma}$)
Stress relaxation (γ)
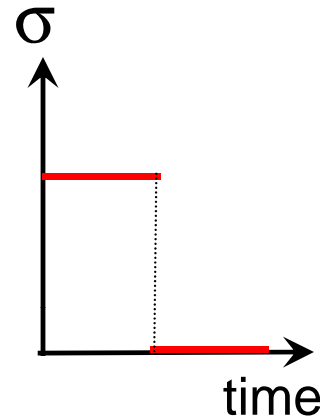
Creep - recovery

Start-up flow
Flow cessation

The response is associated with a non-equilibrium structure
The microscopic interpretation/modelling is difficult
It is generally necessary to determine the dynamic structure
Flow heterogeneities are frequent

Problems and challenges

The torque falls outside the experimental window (0.02 μN.m/200 mN.m in general)

Evaporation

Phase separation, sedimentation…

Incorrect loading

The edge of the sample develops an elastic instability

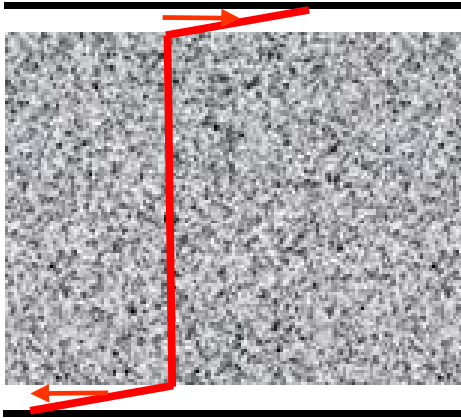The materials stores internal stresses that slowly relax

Non homogeneous flows

Slow relaxation in a concentrated suspension

$\phi \cong 0.80$

$$\sigma = \sigma_{\mathrm{i}} \exp\left(-\frac{t - t_0}{\tau_\ell}\right)$$
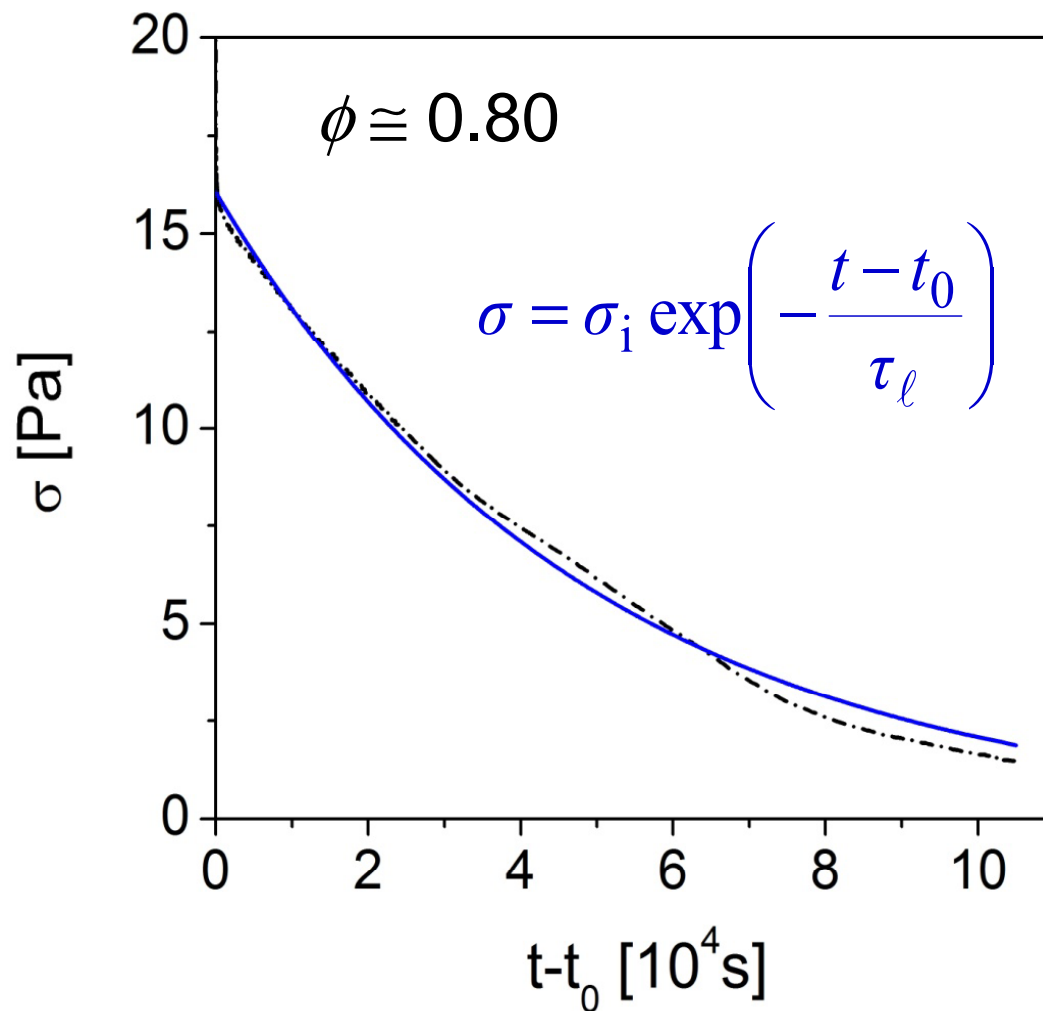
- **Suspension in the jamming regime**

- **Generic behaviour of glassy materials**

- **Sequences of measurements are impossible unless the sample is annealed**

Mohan, L., R. T. Bonnecaze, M. Cloitre, Phys. Rev. Lett. 111, 268301 (2013)

Non homogeneous flows

Wall slip

Shear-banding

Continuous shear-banding

Polymer melts
Colloidal suspensions
Jammed colloids
Granular materials

Entangled polymers
Star polymers
Giant micelles

Colloidal glasses

Wall slip of jammed suspensions
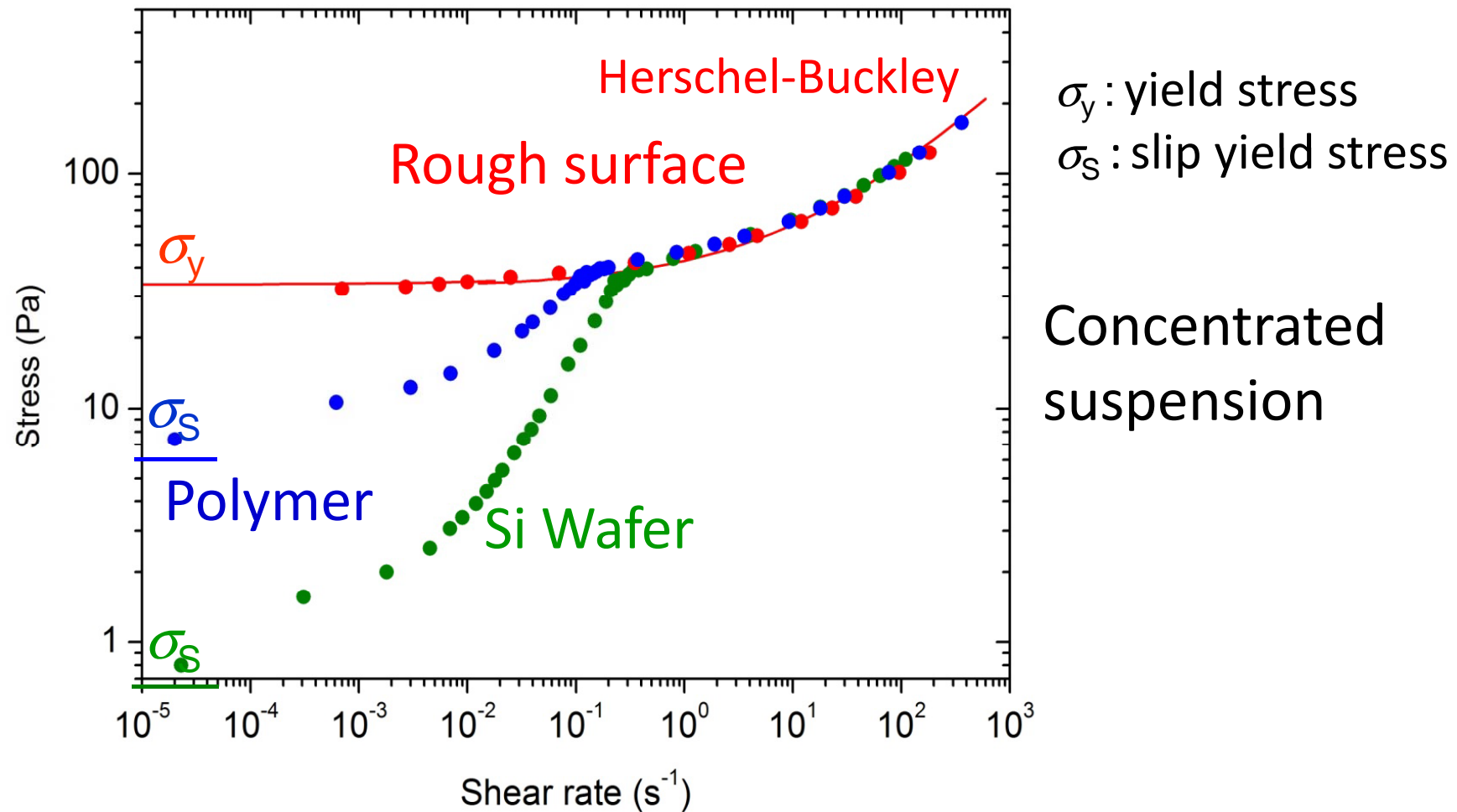
Slip occurs at low shear rates. The importance of slip depends of short range forces between the wall and the particles

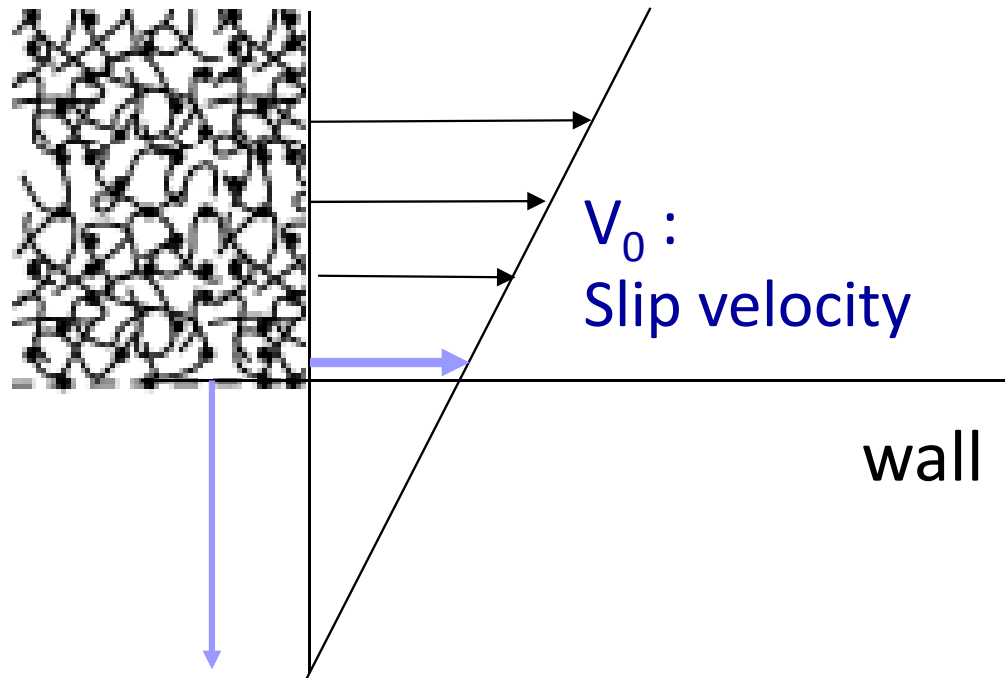# Slip of jammed emulsions: soft lubrication

At rest

$$f^{EHD}\left(\propto \dfrac{\eta_s V R}{E^*}\right)^{1/2}$$

$\vec{f}^{EHD}$

f_n

Osmotic pressure

V

δ
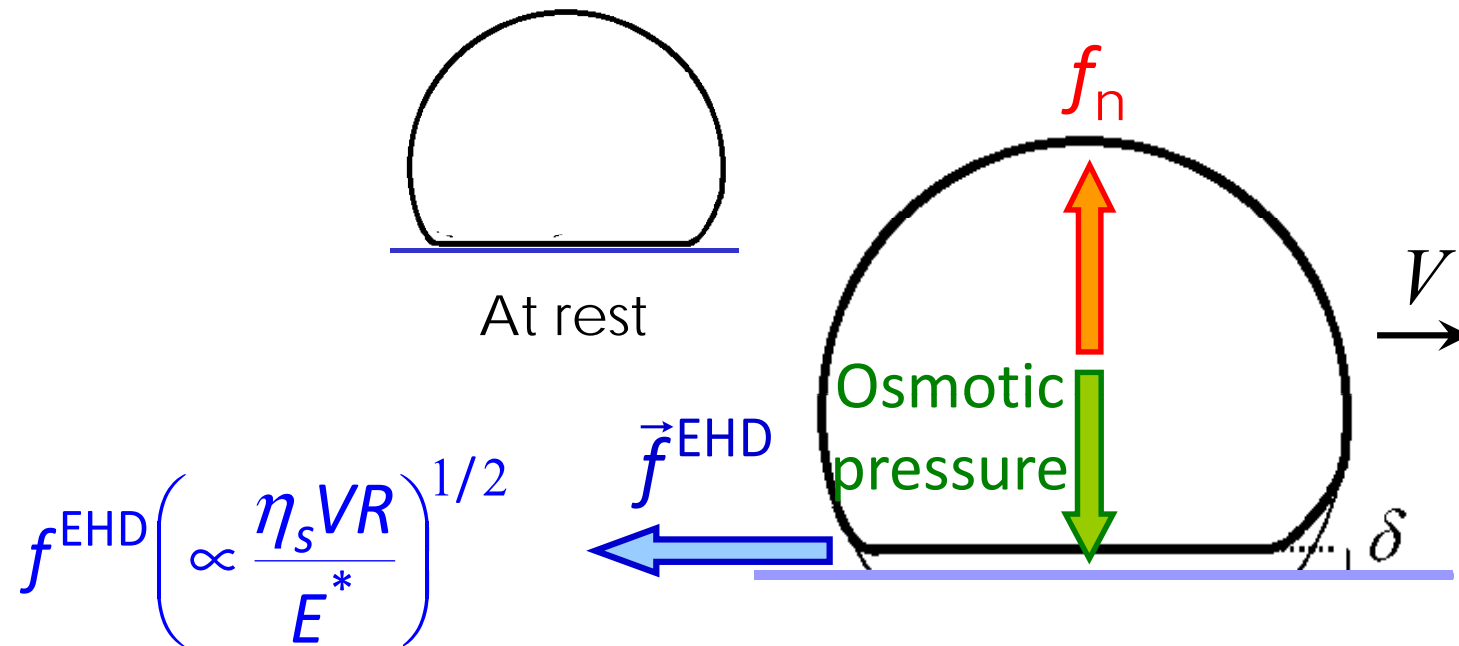
Film thickness : 5 nm − 50 nm

Relative motion causes asymmetry, which generates a lift force (f_n) and maintains a lubricated film

 S. Meeker, R.T. Bonnecaze & M. Cloitre, *Phys. Rev. Lett*. **92**, 198302 (2004)

Slip of polymer melts

Smooth wall without chain adsorption

V_0 :
Slip velocity

wall

ℓ : extrapolation length

• Wall stress

$$\eta_{\text{mono}} \frac{V_0}{a} = \eta \frac{V_0}{\ell}$$

$$\ell \sim \frac{\eta}{\eta_{\text{mono}}} a \sim \frac{N^3}{N_e^2} a$$

• Orders of magnitude

$\eta \sim 10^4$ Pa.s
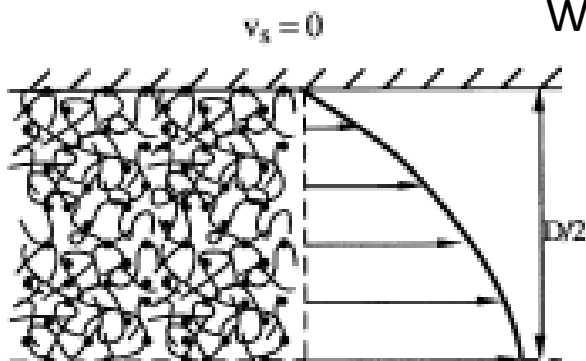$\eta_{\text{mono}} \sim 10^{-3}$ Pa.s
$a \sim 10^{-9}$ m
(monomer size)
$\ell \sim 1$ cm !
Wall slip

(P.G. de Gennes 79)

Chains adsorbed at the wall

II

$V \sim \sigma$ I

LDPE linéaire, M_W=114000g/mole
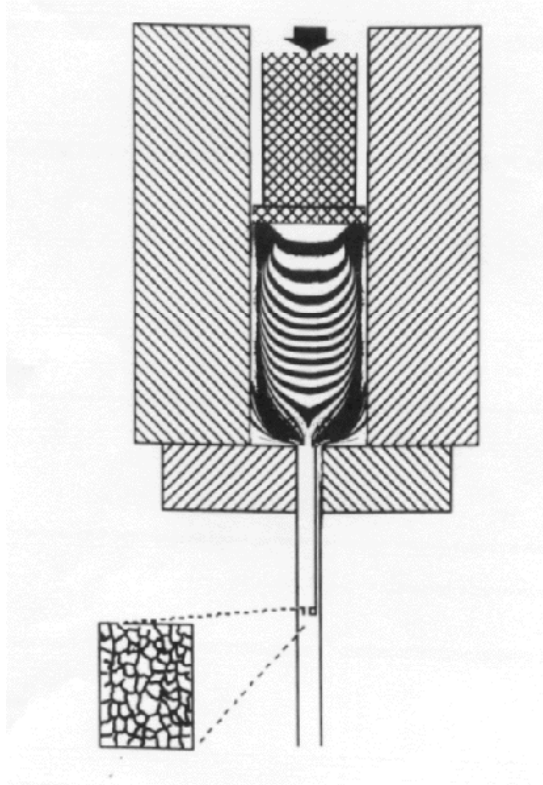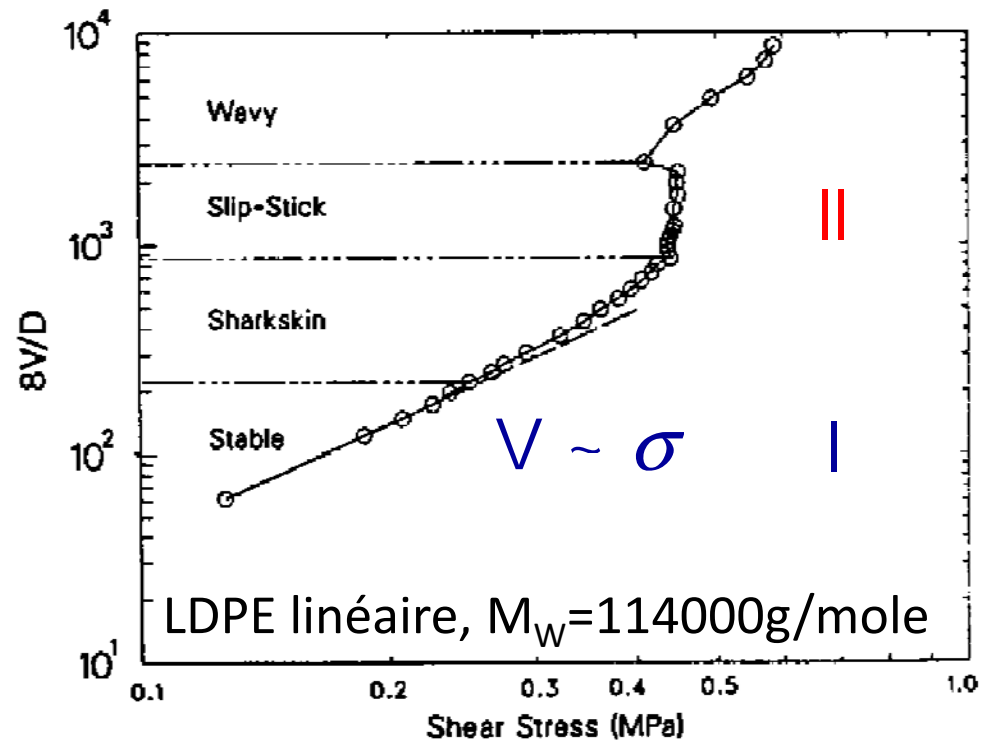
I. Entangled

II. Disentangled (large velocity)

Wang et al, Macromol. 96
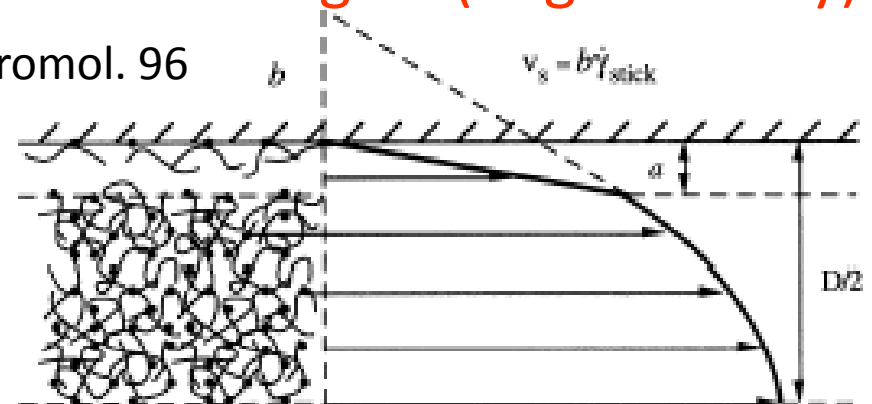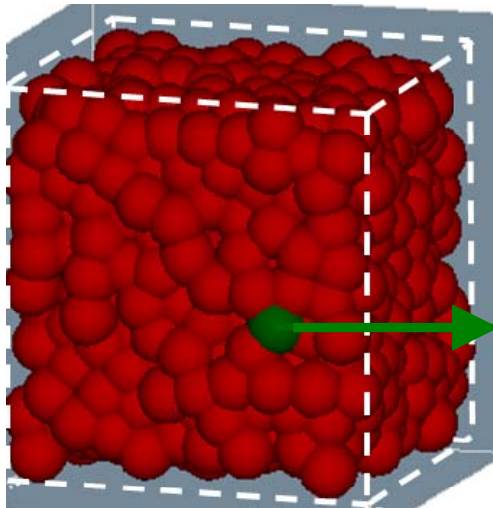
2.2 Rheology at the microscopic scale
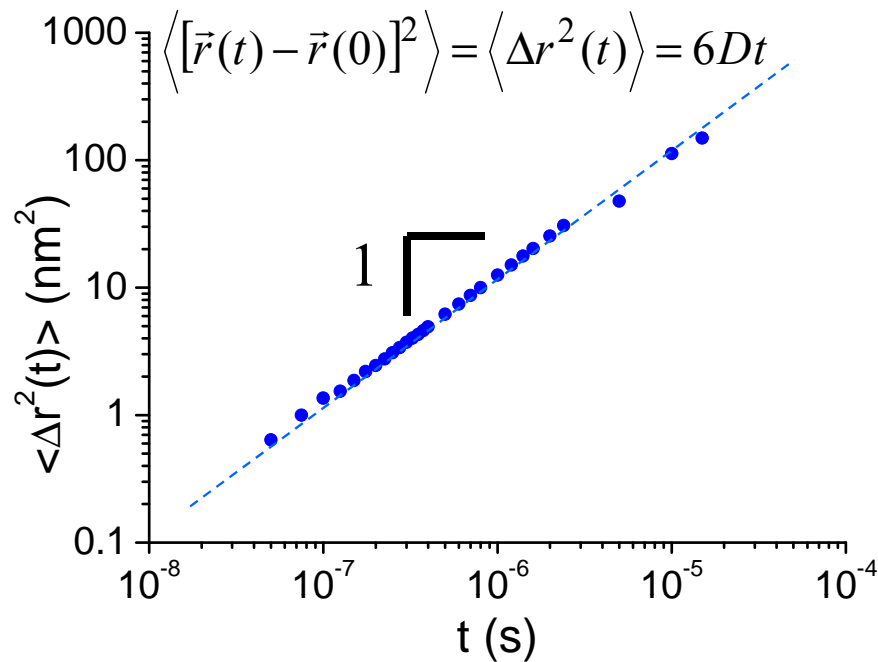
Passive and active microrheology
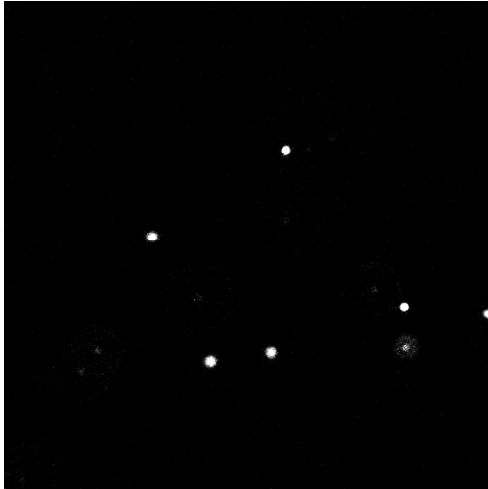
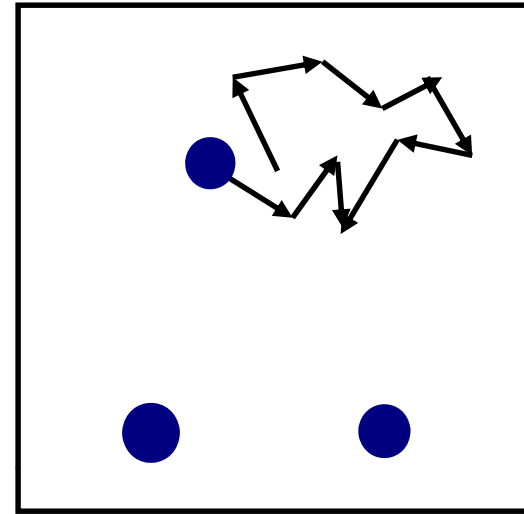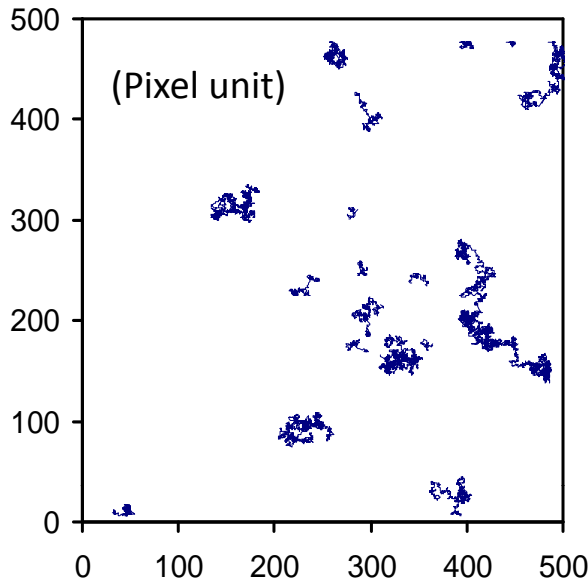Passive μ-rheology: we measure the response to thermal fluctuations of spherical probe colloids ($\cong$ 1 μm) added to the material

Active μ-rheology: we measure the response to a forced excitation (optical or magnetic tweezers) of spherical probe colloids ($\cong$ 1 μm) added to the material
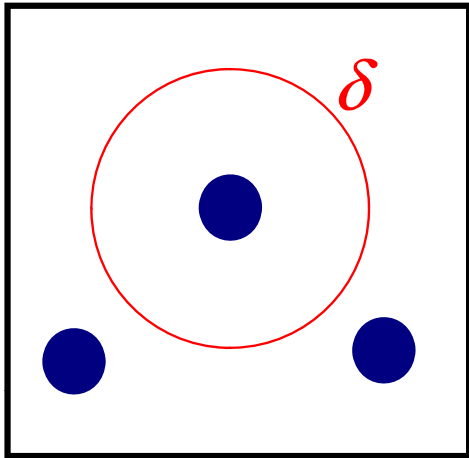
Brownian spheres in a viscous fluid

$$\left\langle [\vec{r}(t) - \vec{r}(0)]^2 \right\rangle = \left\langle \Delta r^2(t) \right\rangle = 6Dt$$

Stokes—Einstein relation
(fluctuation-dissipation) :

$$D = \frac{kT}{\pi \eta R}$$

$$\eta = \frac{kT}{\pi R \dfrac{\left\langle \Delta r^2(t) \right\rangle}{t}}$$

$$G'' = \eta \omega = \frac{kT}{\pi R \left\langle \Delta r^2(1/\omega) \right\rangle}$$
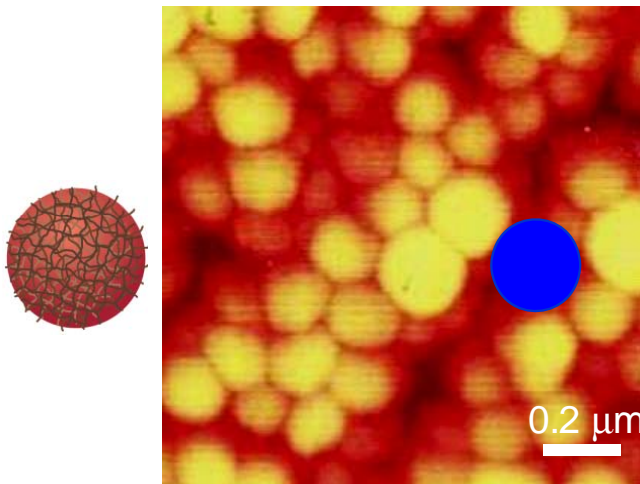
Brownian spheres in an elastic medium

δ

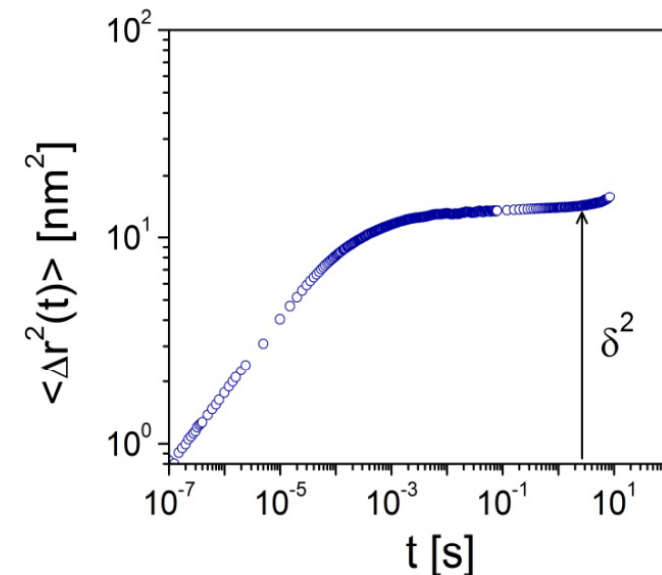The displacement of the sphere is constrained in a volume of radius δ:

$$t \to \infty : \left\langle \Delta r^2(t) \right\rangle \to \delta^2$$

$$G_0 \left(\frac{\delta}{R} \right)^2 R^3 \approx kT \quad \text{or:} \quad G_0 \approx \frac{kT}{R < \Delta r^2(t) >_\infty}$$

(elastic energy~ *kT*)

Jammed microgel suspension

Generalized Stokes-Einstein relation

The relaxation modulus has the same behaviour as the local fluctuations that affect the displacement of the probe particles

$$\widetilde{G}(s) = \frac{kT}{\pi R s < \Delta \widetilde{r}^2(s) >}$$

$\Delta \widetilde{r}^2(s)$ is the Laplace transform of $<\Delta r^2(t)>$

The complex modulus is obtained by making $s = i\omega$ in $\widetilde{G}(s)$

Discrete algorithms have been developed

T. G. Mason and D. A. Weitz, *Optical Measurements of Frequency-Dependent Linear Viscoelastic Moduli of Complex Fluids*, Phys. Rev. Lett. **74**, 1250 (1995)
T. G. Mason, *Estimating the viscoelastic moduli of complex fluids using the generalized Stokes-Einstein relation*, Rheol. Acta **39**, 371 (2000)
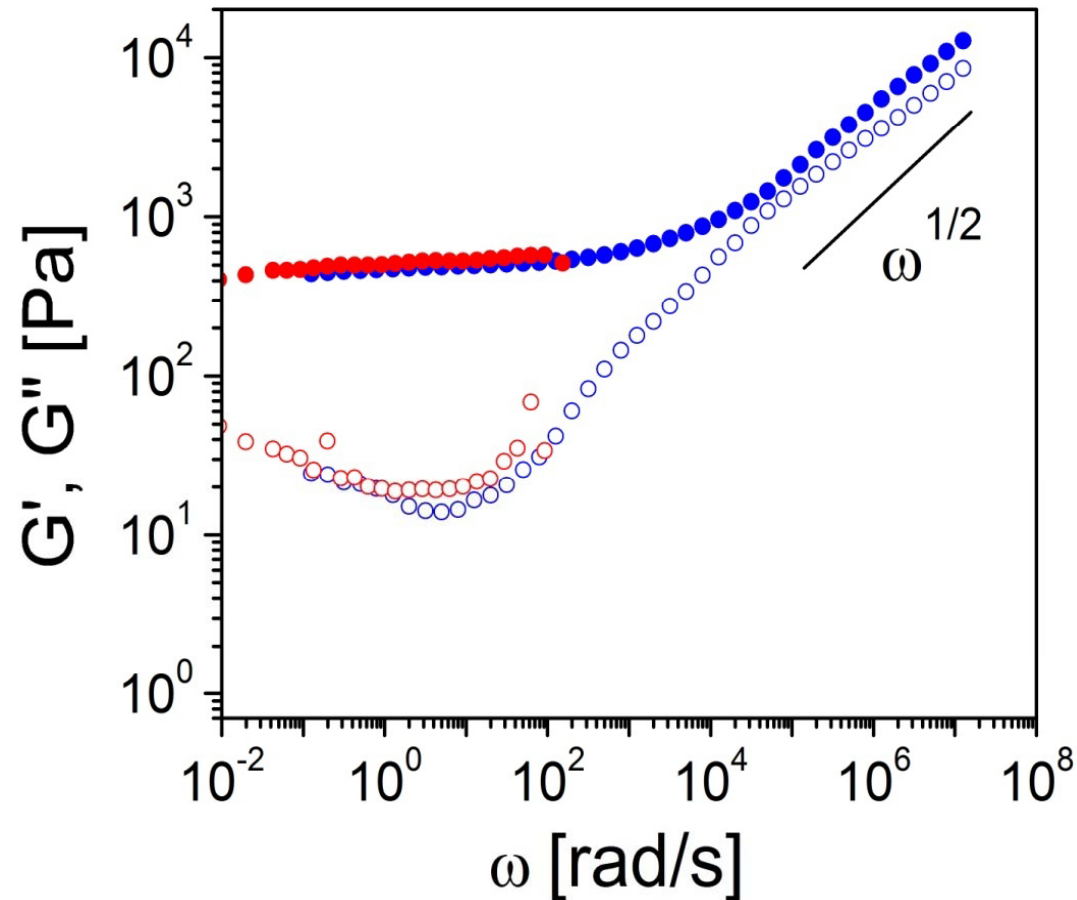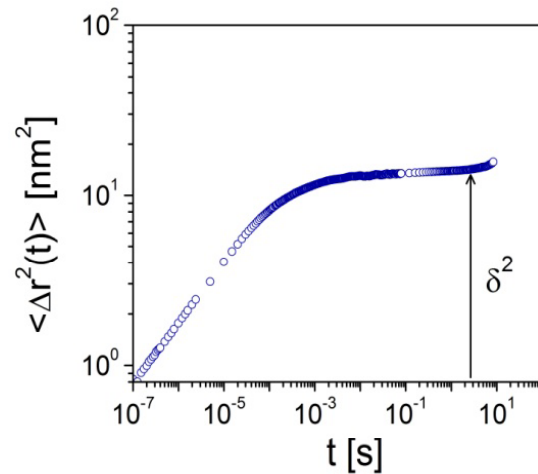
Viscoelastic polymer solution
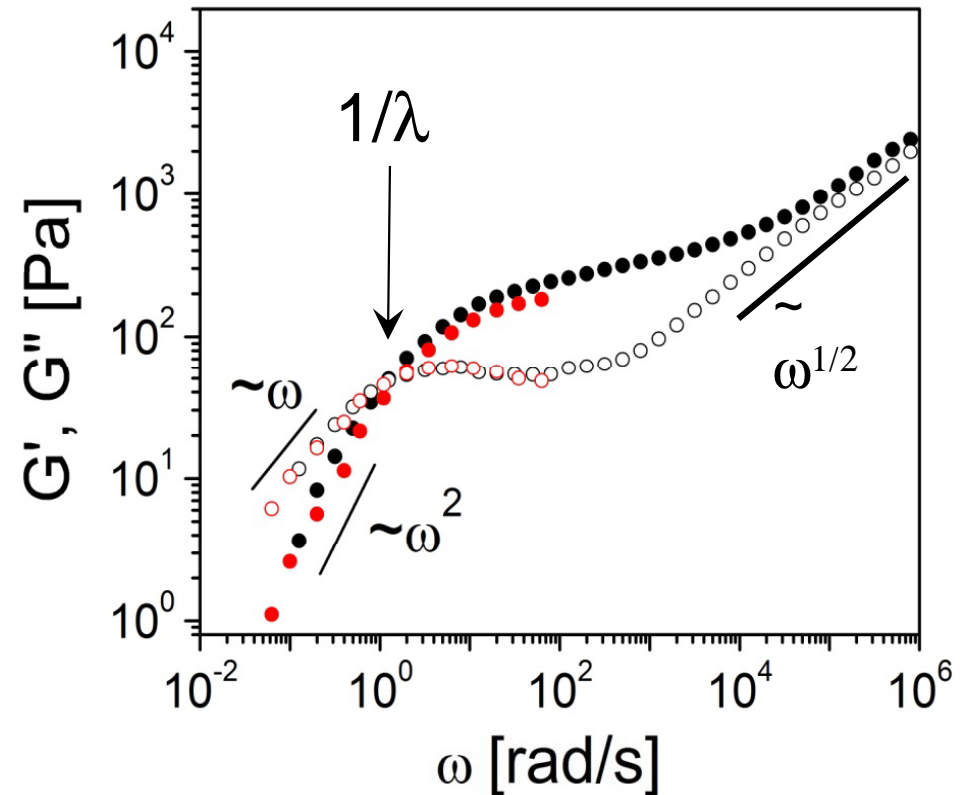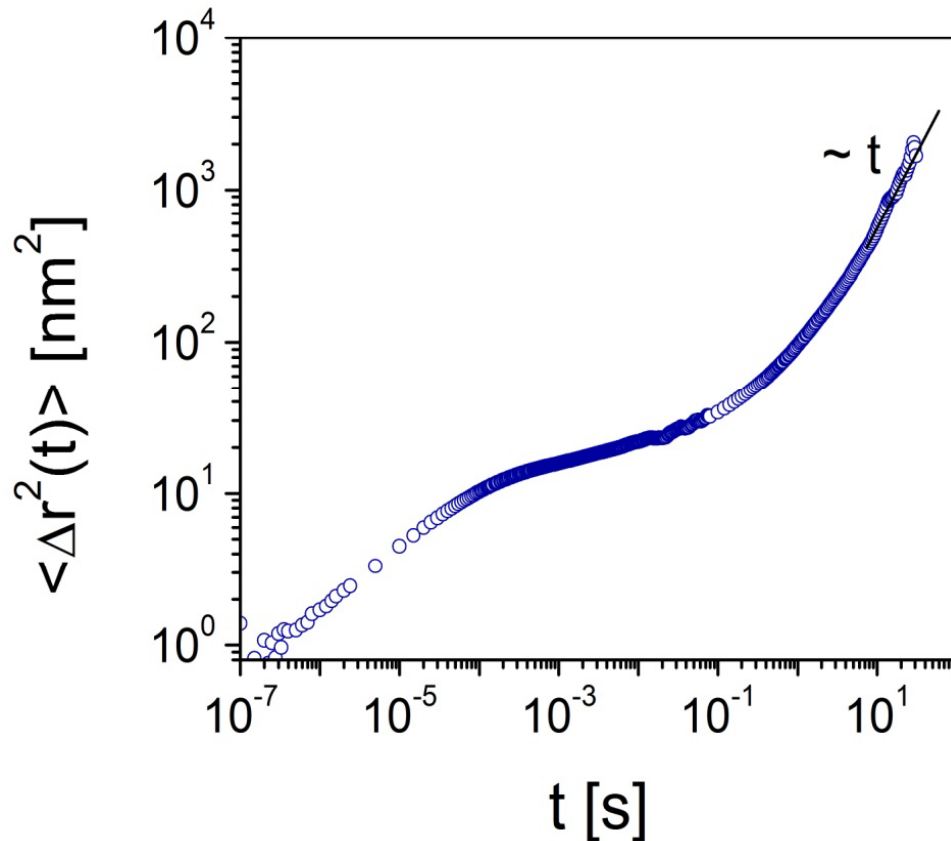
High frequency spectroscopy

F. Monti, *Microrhéologie de suspensions colloïdales non ergodiques: relaxations locales, dynamiques lentes et vieillissement*, PhD thesis, Université Pierre et Marie Curie, Paris (2010)

Linear rheology of a jammed suspensions

F. Monti, *Microrhéologie de suspensions colloïdales non ergodiques: relaxations locales, dynamiques lentes et vieillissement*, PhD thesis, Université Pierre et Marie Curie, Paris (2010)
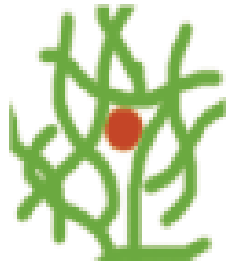
Advantages and limitations

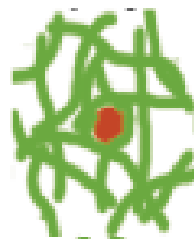Small volumes

Linear response (the excitation is $\cong kT$)

Good sensibility (G' et G" ~ 10^{-2} Pa)

No suitable for rigid materials

The coupling between the probe particles and the environment matters
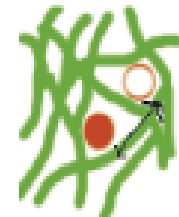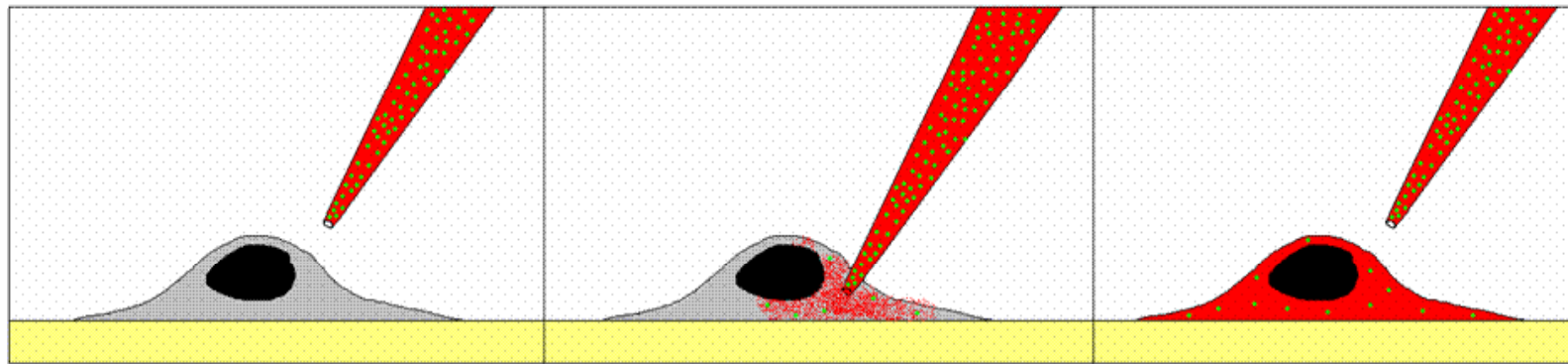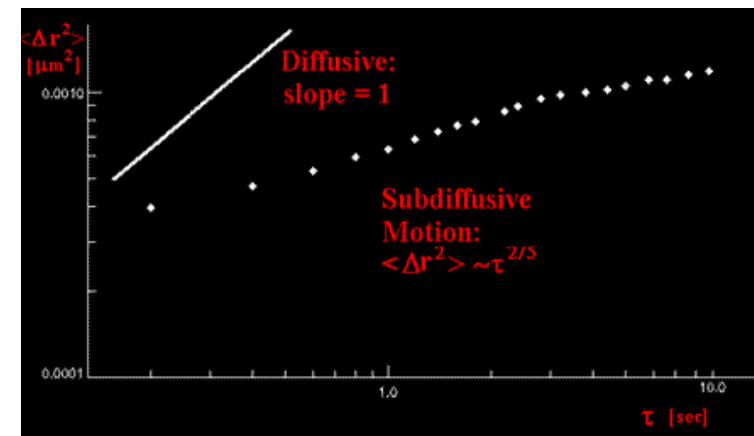

Ideal coupling (neutral)
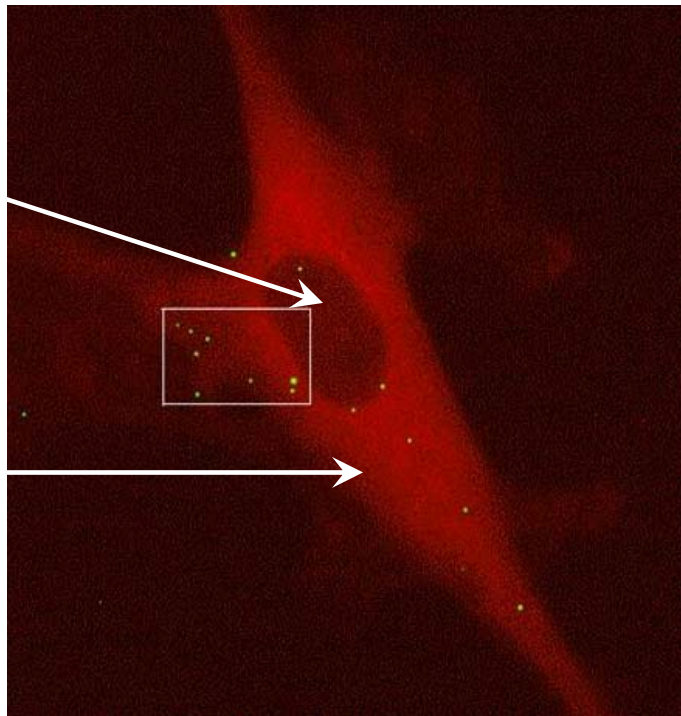
Adsorption　　Depletion　　$R < \xi$
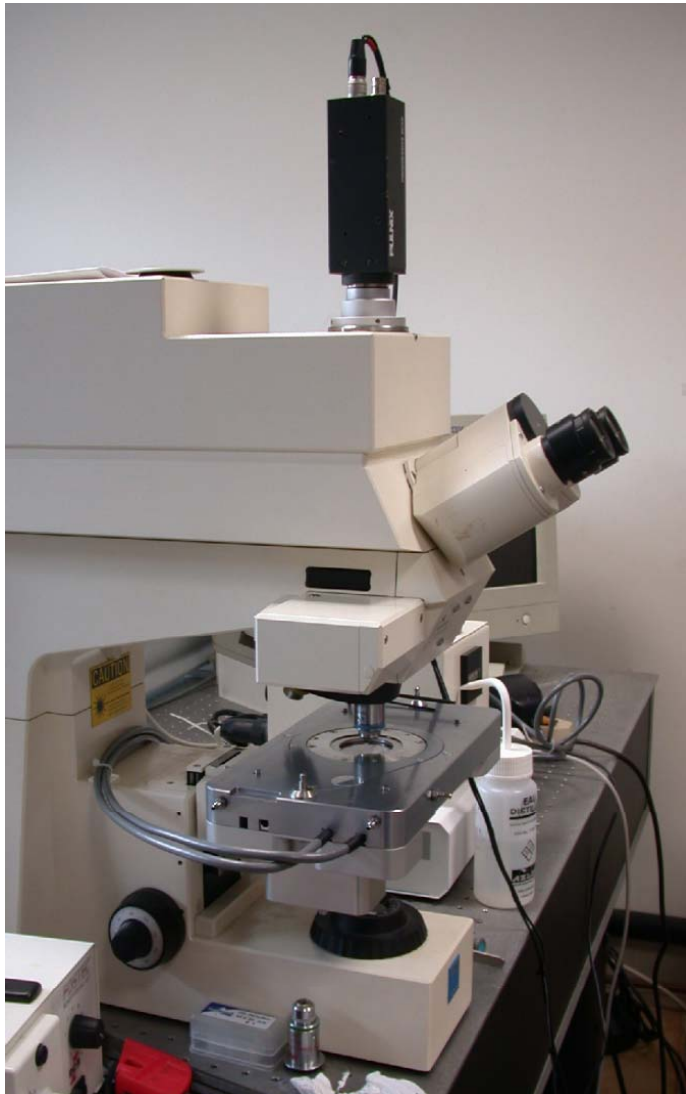
Example: intracellular dynamics

Nucleus

Actin
network

Diffusive: slope = 1

Subdiffusive Motion:
$\langle \Delta r^2 \rangle \sim \tau^{2/3}$
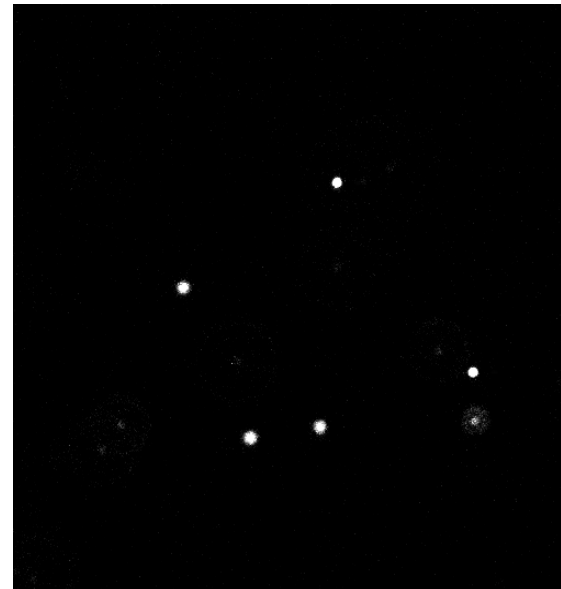
http://www.seas.harvard.edu/projects/weitzlab/research/micrheo.html

Particle tracking by video-microscopy

Experimental setup (MMC lab)
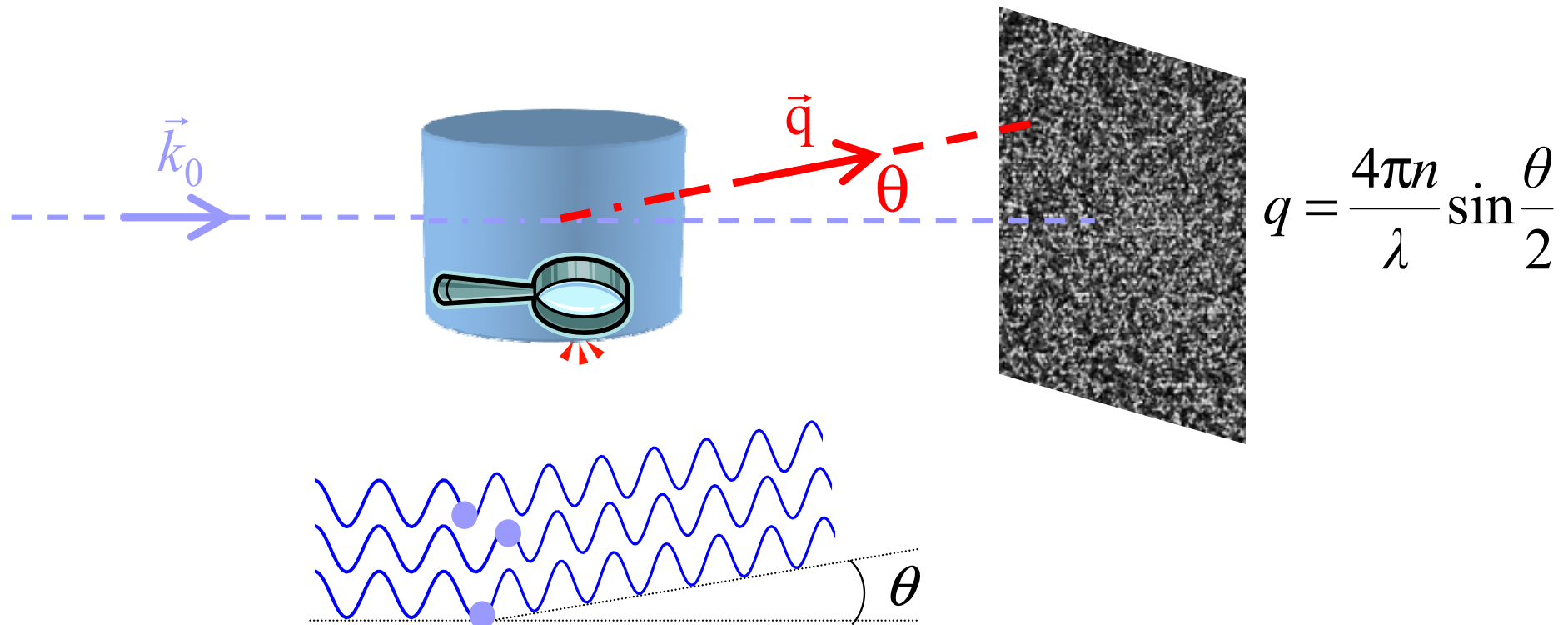
Δx et $\Delta y \cong 0.1$ µm
$\Delta z \cong 1$ µm

Spatial resolution
0.01 s$< \tau <100$ s

Raw   Threshold   Segmentation

34 J. C. Crocker and D. G. Grier, *Methods of digital video microscopy for colloidal studies*", J. Colloid Interface Sci. **179**, 298 (1996)
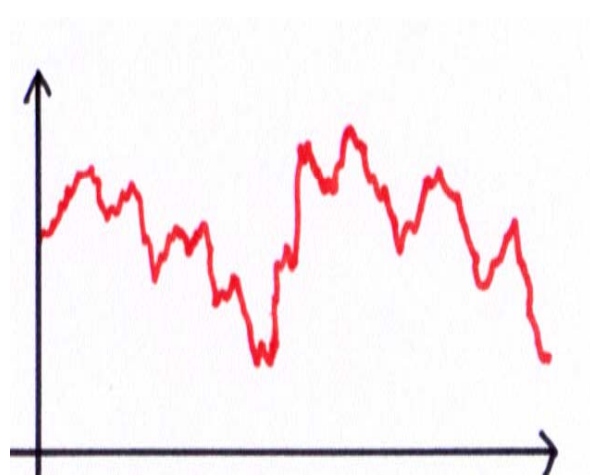
Light scattering

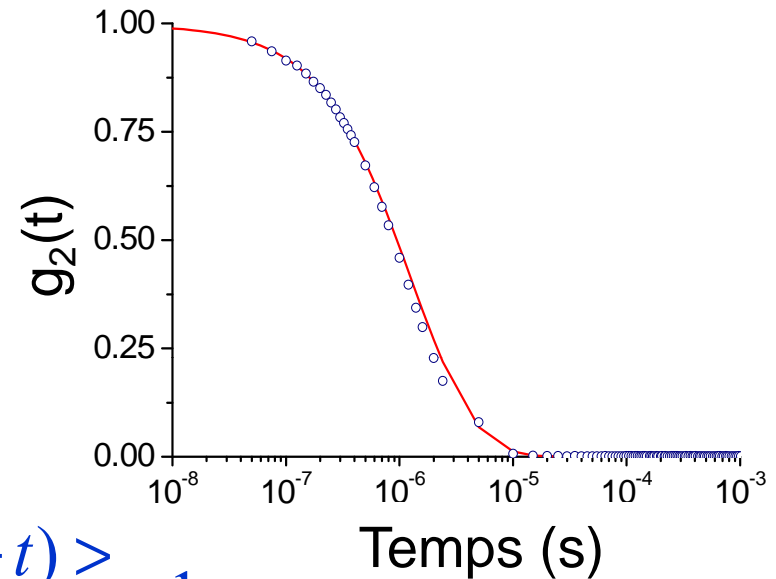$$q = \frac{4\pi n}{\lambda} \sin \frac{\theta}{2}$$
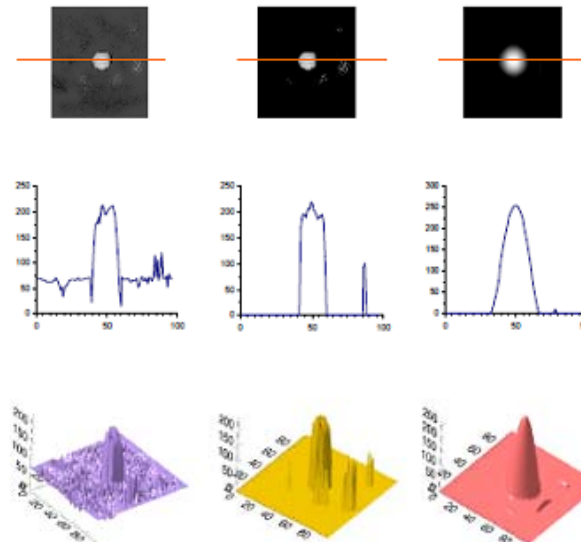
Interferences between photons scattered by the particles in the scattering volume produce a speckle pattern which fluctuates in the course of time

Simple diffusion limit where each photon has been scattered once
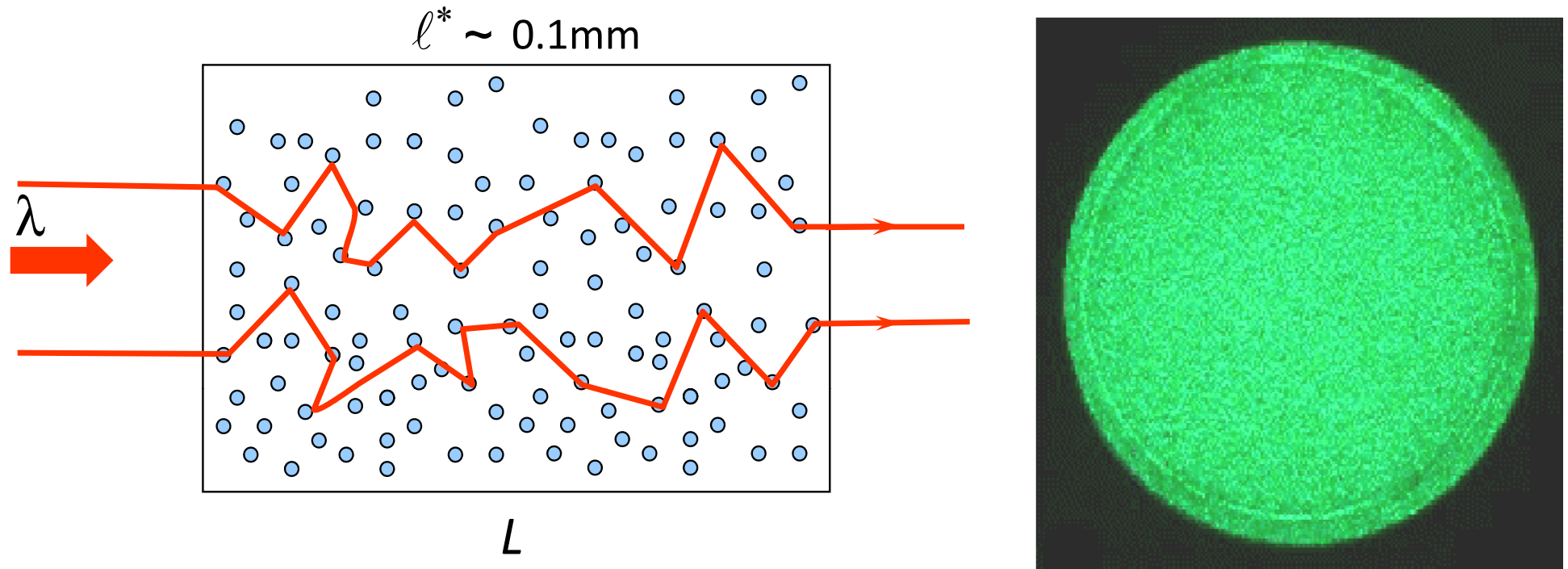
Computing $<\Delta r^2(t)>$

Autocorrelation

$$g_2(t) = \frac{<I(t_0)I(t_0+t)>}{<I(t_0)>^2} - 1$$

$g_2(t)$ is related to the mean-square displacement

$$g_2(t) = \exp\left(-\frac{q^2 <\Delta r^2(t)>}{3}\right)$$

Spatial sensitivity : $<\Delta r^2(t)> \sim \lambda^2$ (typically 0.1 µm²)

Multiple light scattering in turbid media

$\ell^* \sim 0.1\text{mm}$

L

Photons execute a random walk

Each photon is scattered many times: $N \sim (L/\ell^*)^2$

Spatial sensitivity: $\langle \Delta r^2(t) \rangle \sim \lambda^2/N$ (typically 1 nm²)
Very short times, i.e. high frequencies, are accessible

Expressions of $g_2(\langle \Delta r^2(t) \rangle)$ depend on the geometry (transmission, backscattering)

37 D. Weitz and D. Pine, *Diffusing Wave Spectroscopy,* in *Dynamic Light Scattering*, Edited by W. Brown, Clarendon Press, Oxford, 1993

Limitations of scattering techniques

1- Averaging time

Proper averaging requires n = 1000 events. To access t_{max}= 100 s, experiments as long as $10^2 \times 10^3 = 10^5$ s (30 h) are required!
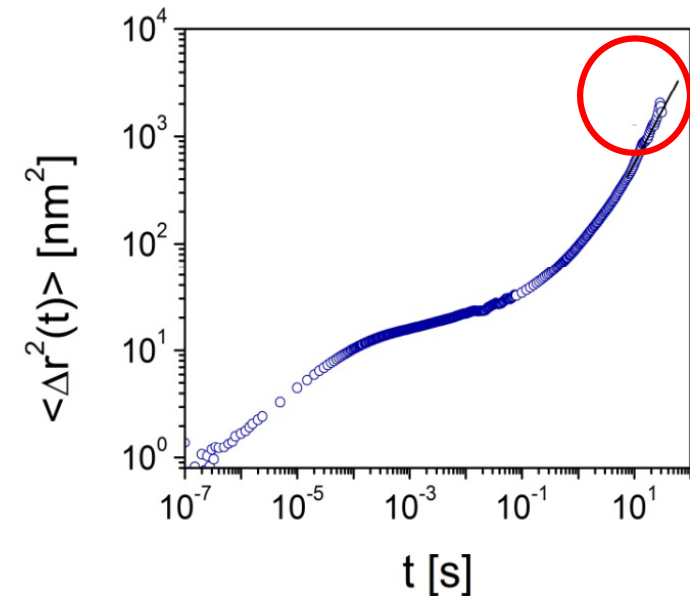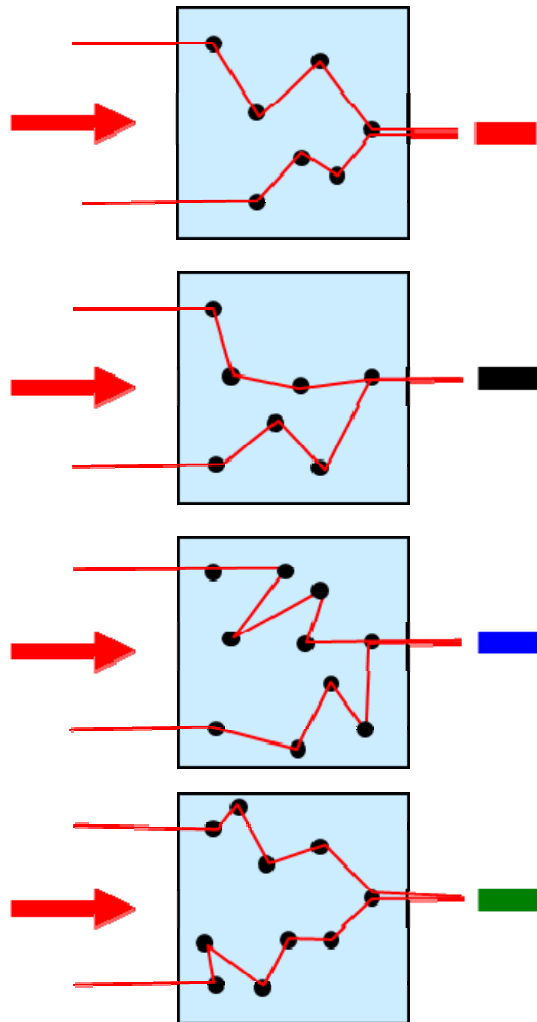

2- Slowly evolving materials in case of aging, aggregation, phase separation.
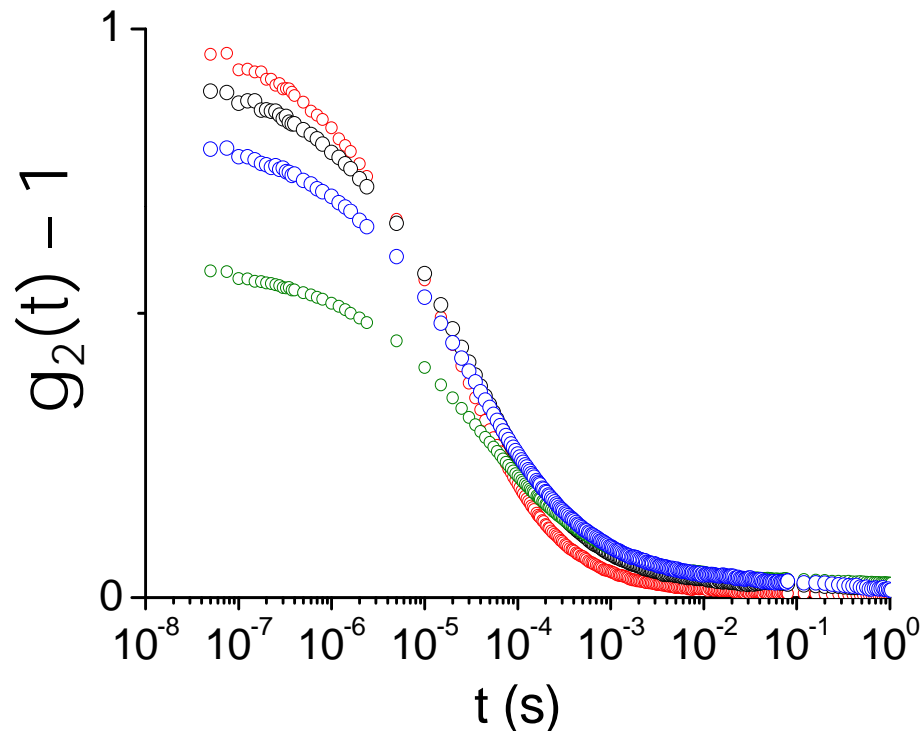
3- Non ergodic materials

4- Presence of spatial heterogeneities (rheo-DLS and rheo-DWS)
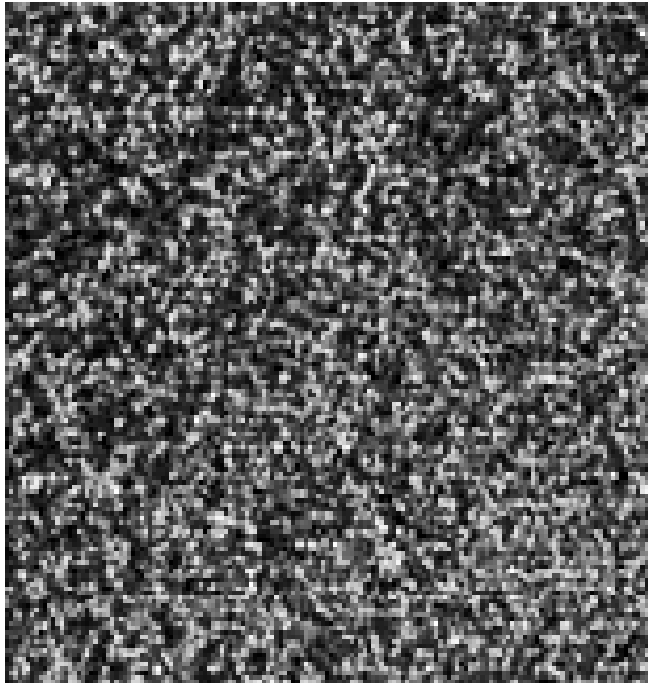
Non-ergodicity

In non-ergodic materials, probe particles are frozen in non-equilibrium configurations

Time-averaged correlation functions depend of observation volume
Efficient protocol to get the ensemble-averaged correlation function?

Multispeckle scheme
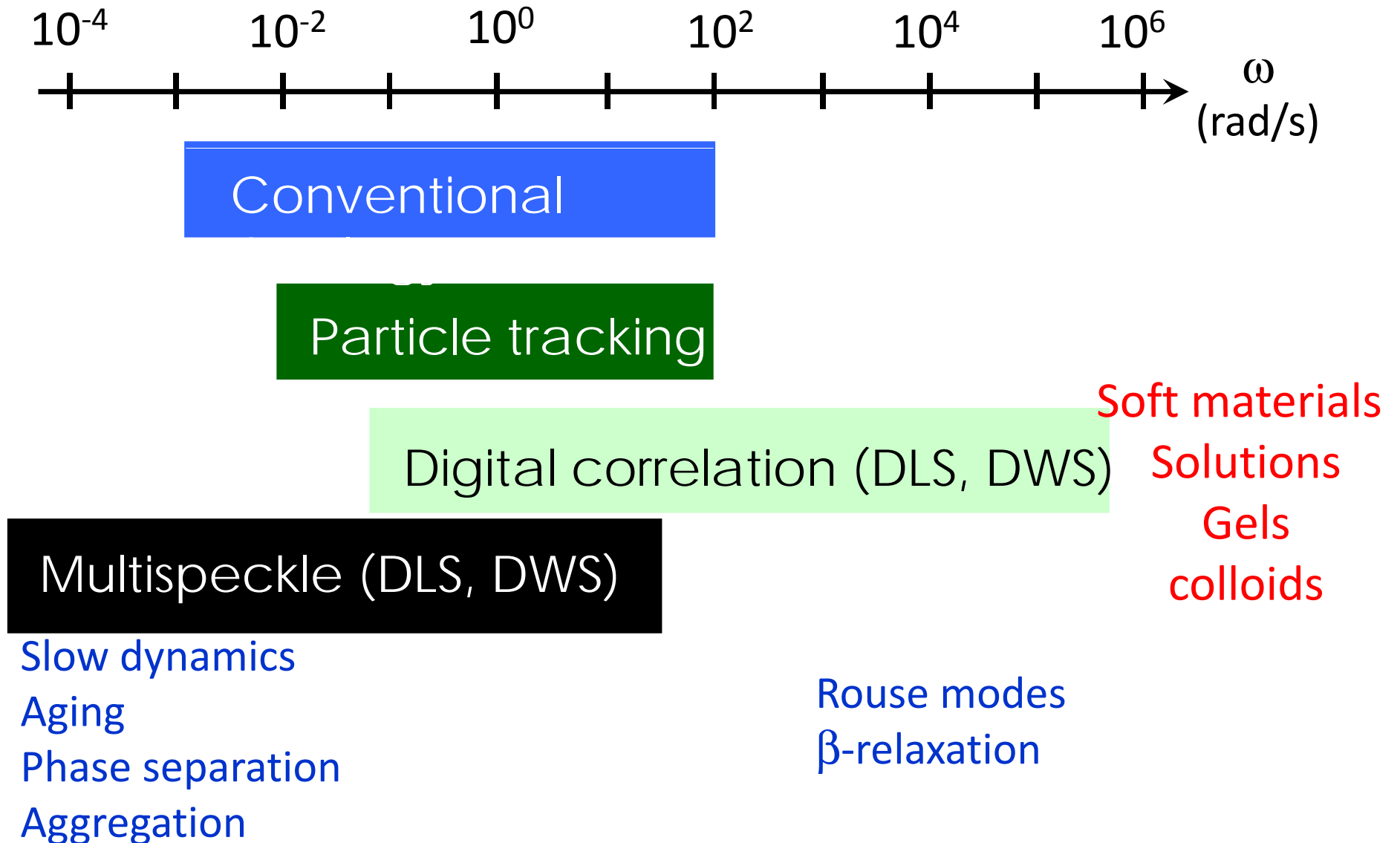

2D speckle patterns are imaged on a CCD camera

Each speckle is considered as an independent detector

Ensemble-averaged correlation function is calculated by averaging time correlation functions over a great number of speckles:

$$g_2(t) - 1 = \frac{\left\langle I_p(t_0) I_p(t_0 + t) \right\rangle_{p,t}}{\left\langle I_p(t_0) \right\rangle_{p,t}^2} - 1$$

L. Cipelletti and D. A. Weitz, *Ultralow-angle dynamic light scattering with a charge coupled device camera based multispeckle, multitau correlator*, Rev. Sci. Instrum. **70**, 3214 (1999)

Summary

10^{-4} 10^{-2} 10^{0} 10^{2} 10^{4} 10^{6}

ω (rad/s)

Conventional

Particle tracking

Digital correlation (DLS, DWS)

Multispeckle (DLS, DWS)

Soft materials
Solutions
Gels
colloids

Slow dynamics
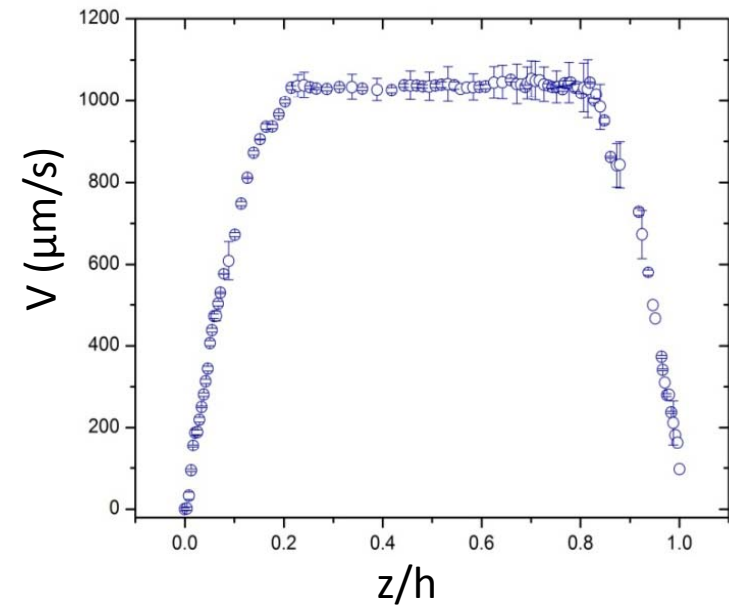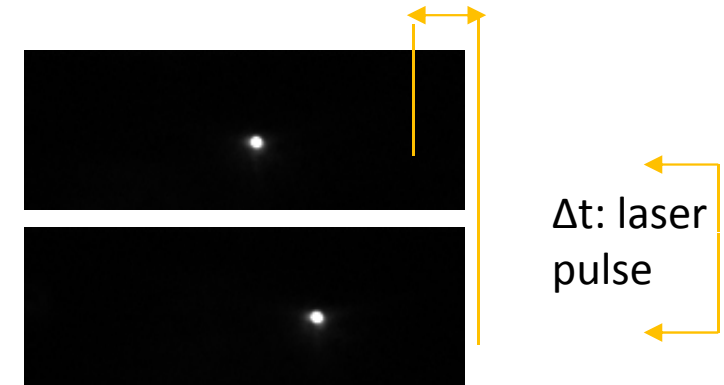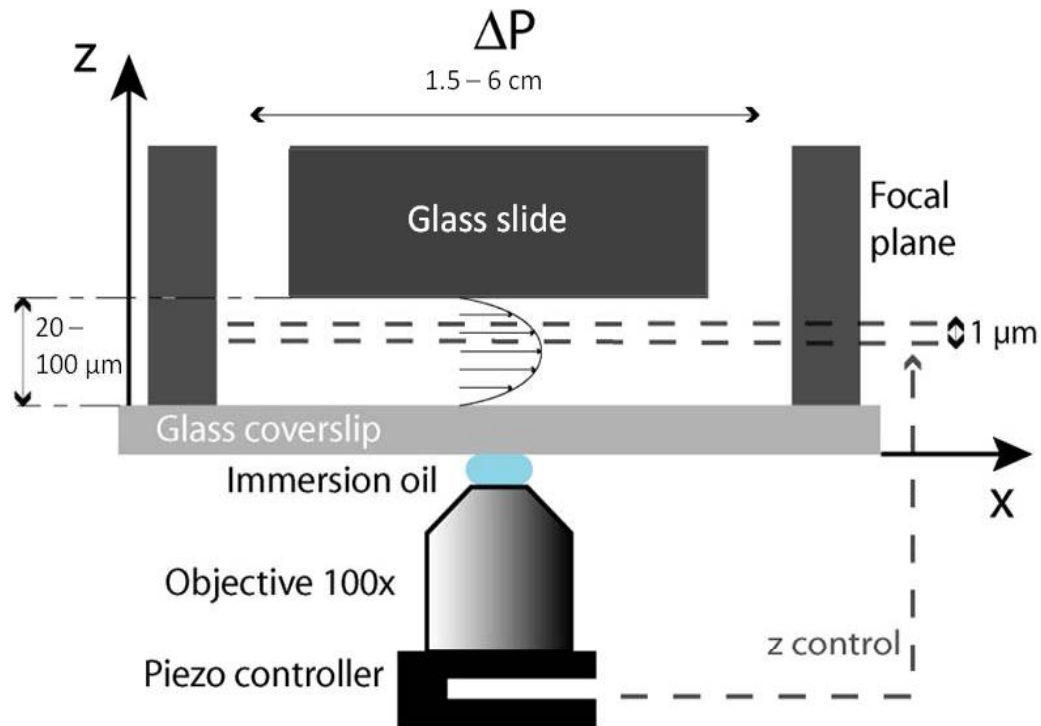Aging
Phase separation
Aggregation

Rouse modes
β-relaxation

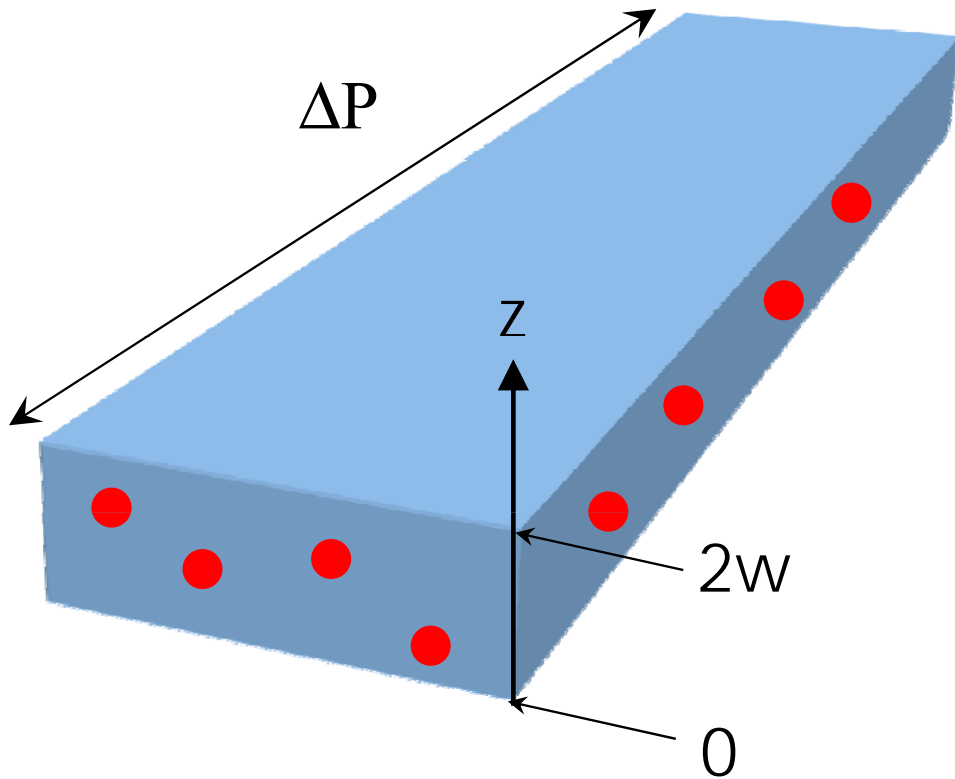# 2.3 Microfluidic techniques

Particle image velocimetry

Small volume
Laminar flows
Local measurements
High shear rates
Integration in microfluidic chips

Particle tracking in a microchannel

At each location z:

➢ PIV or PTV gives V(z)

$$\dot{\gamma}(z) = \frac{V(z+dz) - V(z-dz)}{2dz}$$

➢

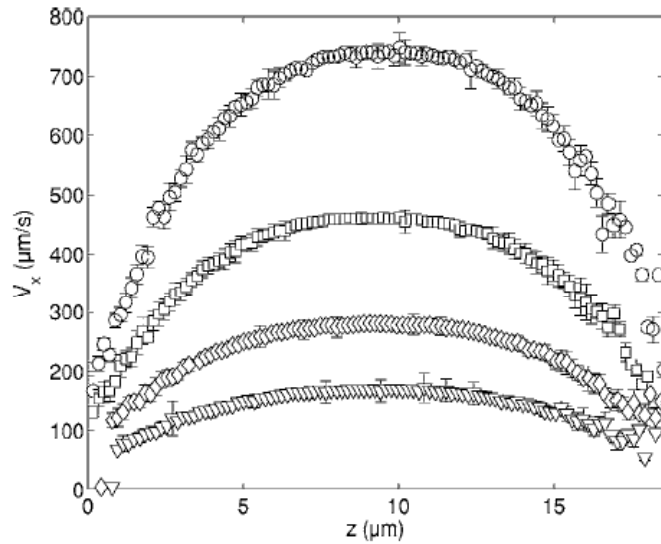$$\sigma(z) = \frac{\Delta P}{L}(z - w)$$

Velocity profile and flow curve

FIG. 2. Velocity profiles for a PEO solution (M_w=5.10⁶ g/mol, C=7.5 g/L) at 27 °C for different pressure drops: (◯) 122 mbars, (□) 96 mbars, (◇) 71 mbars, and (▽) 52 mbars. The profiles have been measured in that order in a single experiment (total duration of 90 min) at the center of a 1.55 cm long and 18±.05 μm thick PDMS on a glass microchannel. The glass wall is located at z=0 with $a \sim 200$ nm precision. The locus of the PDMS wall, away from the optics, is less precise.
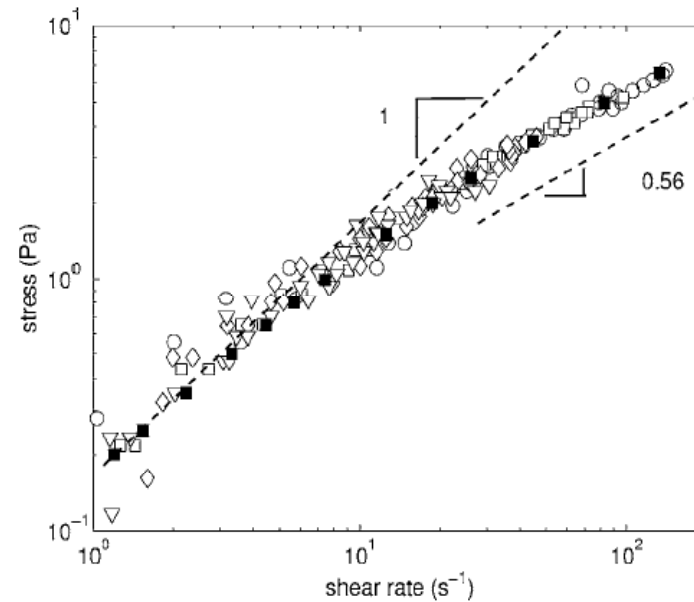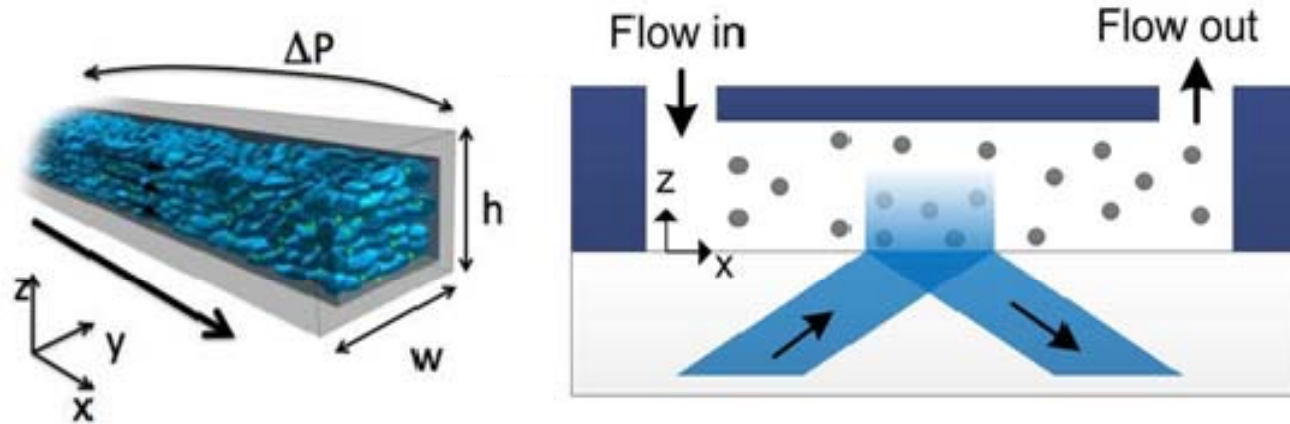
FIG. 3. Stress vs strain rate curve extracted from the velocity profiles of Fig. 2 (same symbols) using the procedure described in the text. The filled squares are independent measurements performed using a Couette rheometer.

G. Degré, P. Joseph, P. Tabeling, S. Lerouge, M. Cloitre & A. Ajdari, *Appl. Phys. Lett.* 89, 024104 (2006)
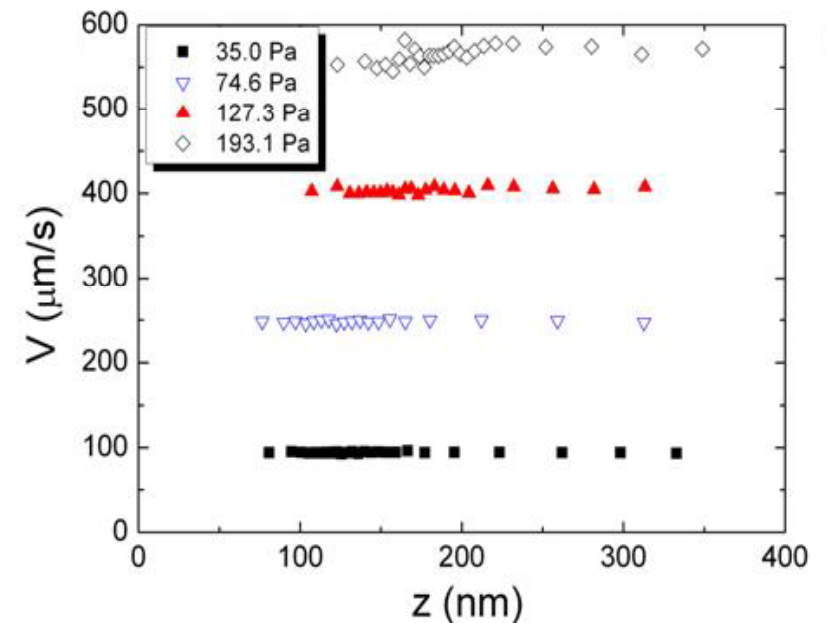
Nanoparticle image velocimetry
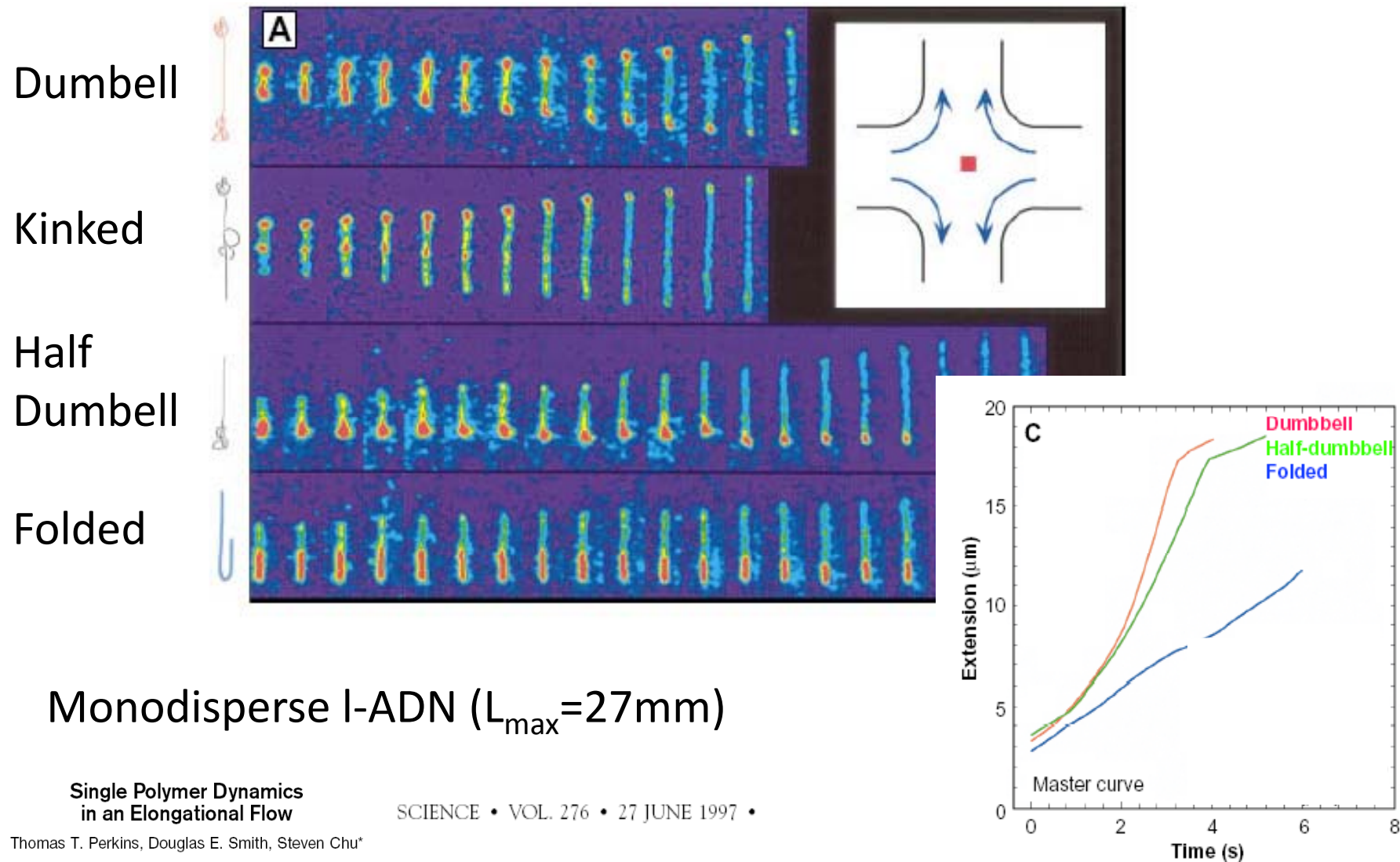

Microfluidic channel

Evanescent waver

Concentrated suspension

Slip occurs in a very thin layer near the wall < 100 nm

P. Joseph and P. Tabeling, *Direct measurement of the apparent slip length*, Phys. Rev. E **71**, 035303, 2005

Conformation of molecules in elongational flows

Dumbell

Kinked

Half Dumbell

Folded

Monodisperse l-ADN (L_{max}=27mm)

Single Polymer Dynamics
in an Elongational Flow

SCIENCE • VOL. 276 • 27 JUNE 1997 •

Thomas T. Perkins, Douglas E. Smith, Steven Chu*
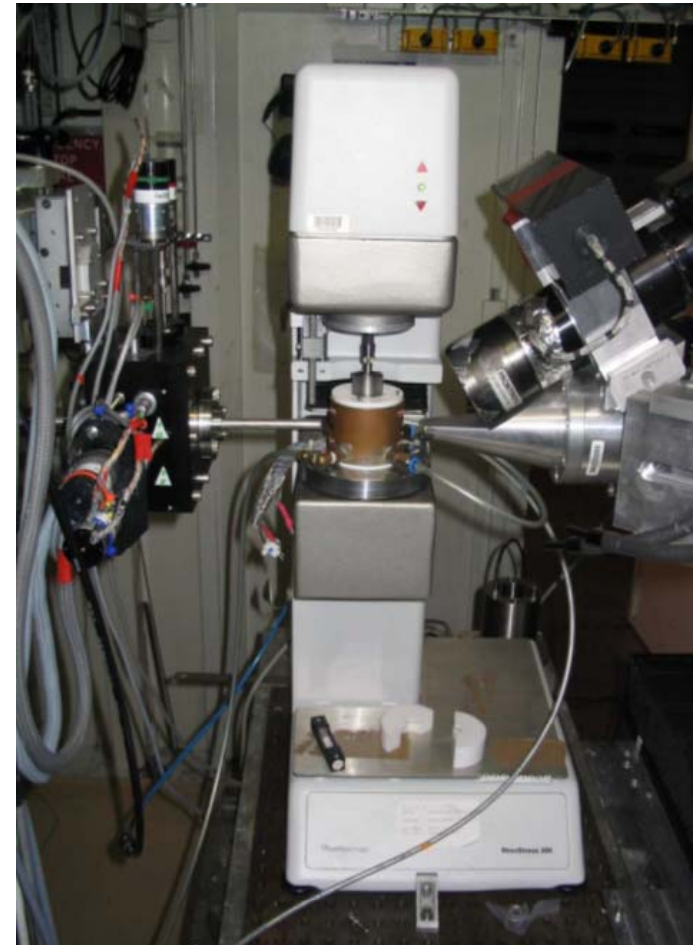
2.4 Rheology and structure

Rheo-SAXS, SANS, DLS

Investigate the structure during flow using SAXS, SANS, and DLS

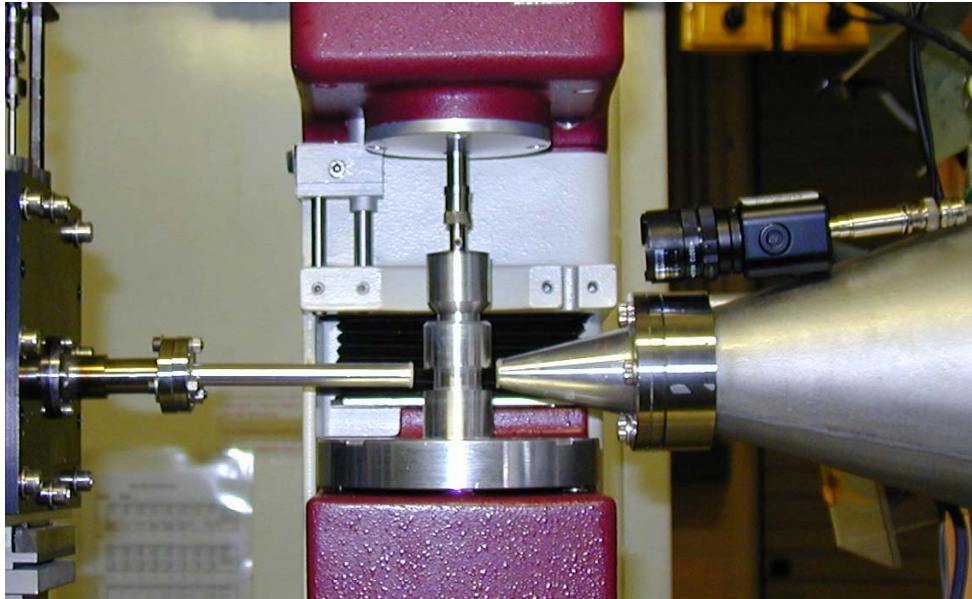A wide range of length scales can be probed:
10-300 nm for SANS and SAXS
50 nm – 10 μm for DLS

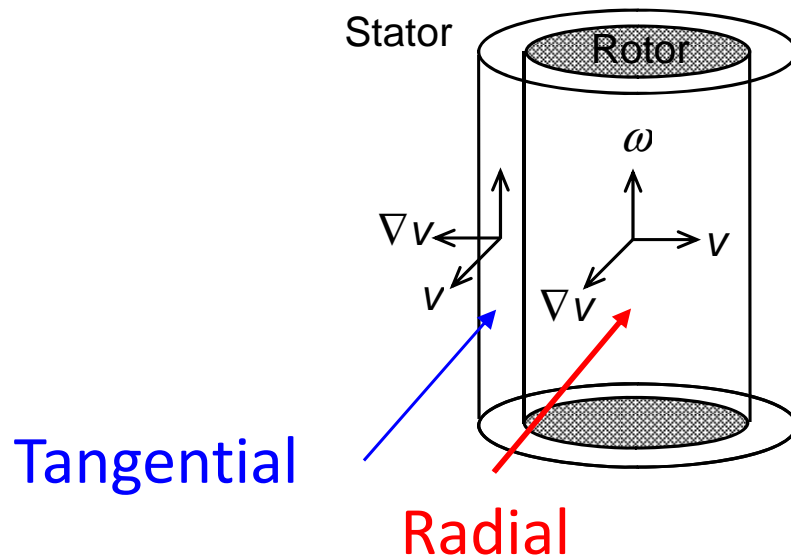Experimental setups and environments begin to be commercially available

Rheo SAXS at ID2 (ESRF)

Dynamics of triblock copolymer solutions

Polystyrene-*b*-polybutadiene-*b*-polymethylmethacrylate (SBM) copolymers in good solvent

- Beam size : $a \cong 300\ \mu m$
- Scan of gap is possible
- Time-resolved experiments
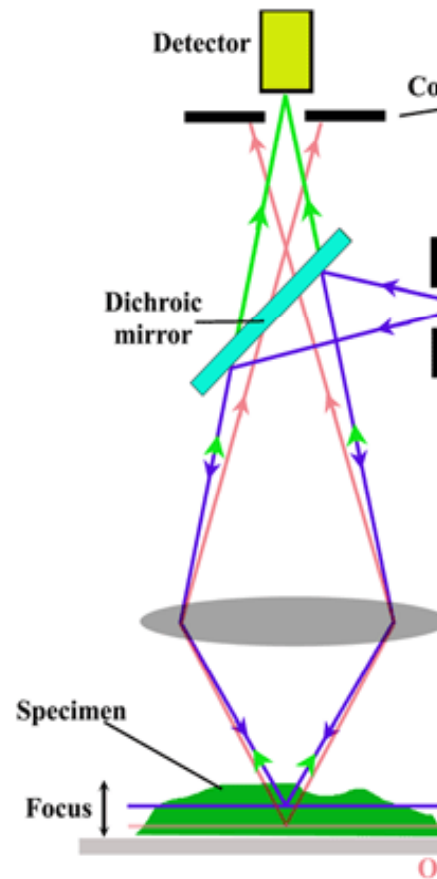 (exposure time as low as 10ms)
- Radial and tangential observation
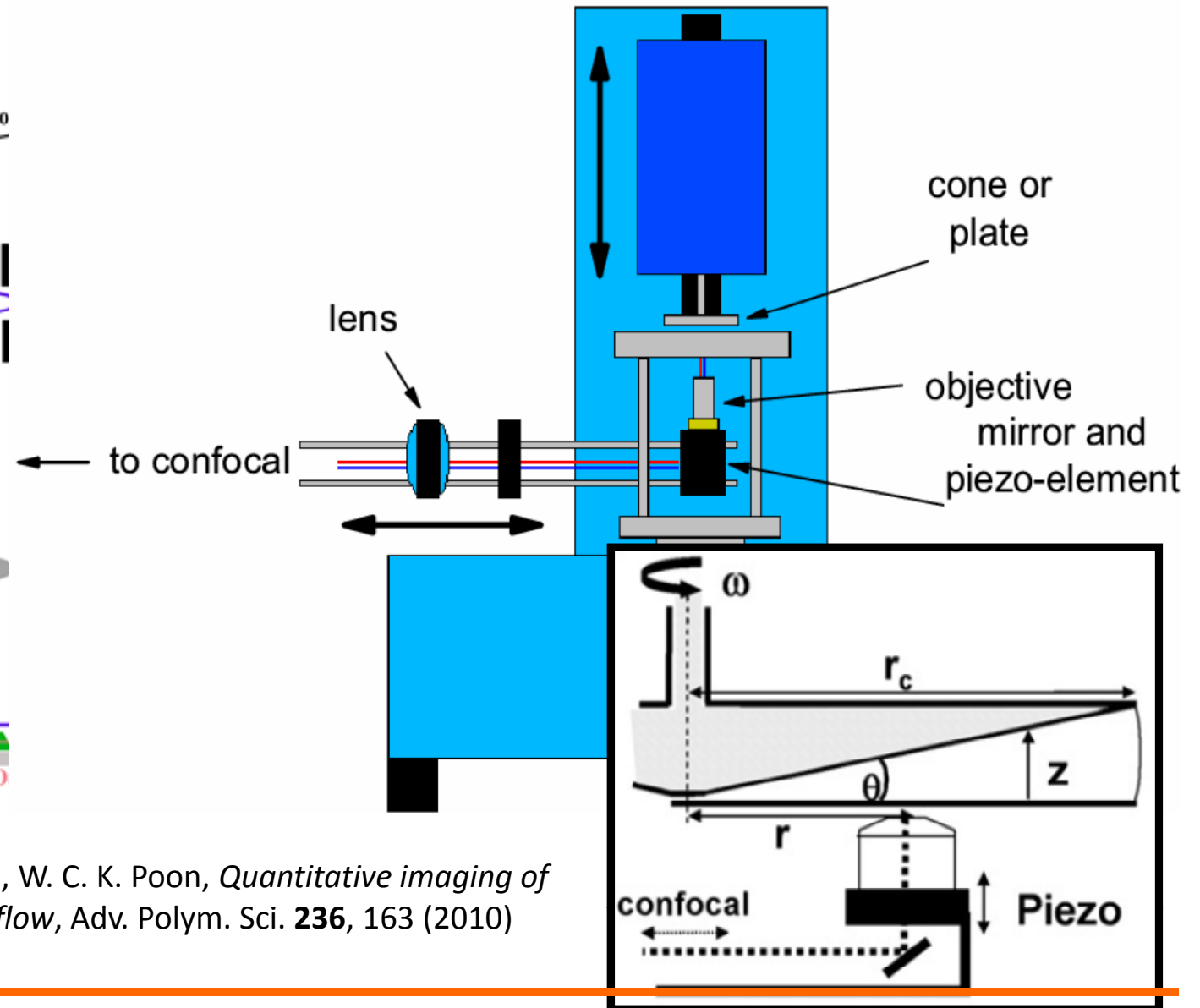
Dynamic orientation diagram of SBM lamellae

Parallel orientation with defects

Viscosity(Pa.s) vs $\dot{\gamma}(\text{s}^{-1})$

Perpendicular orientation

$1/\tau_c$
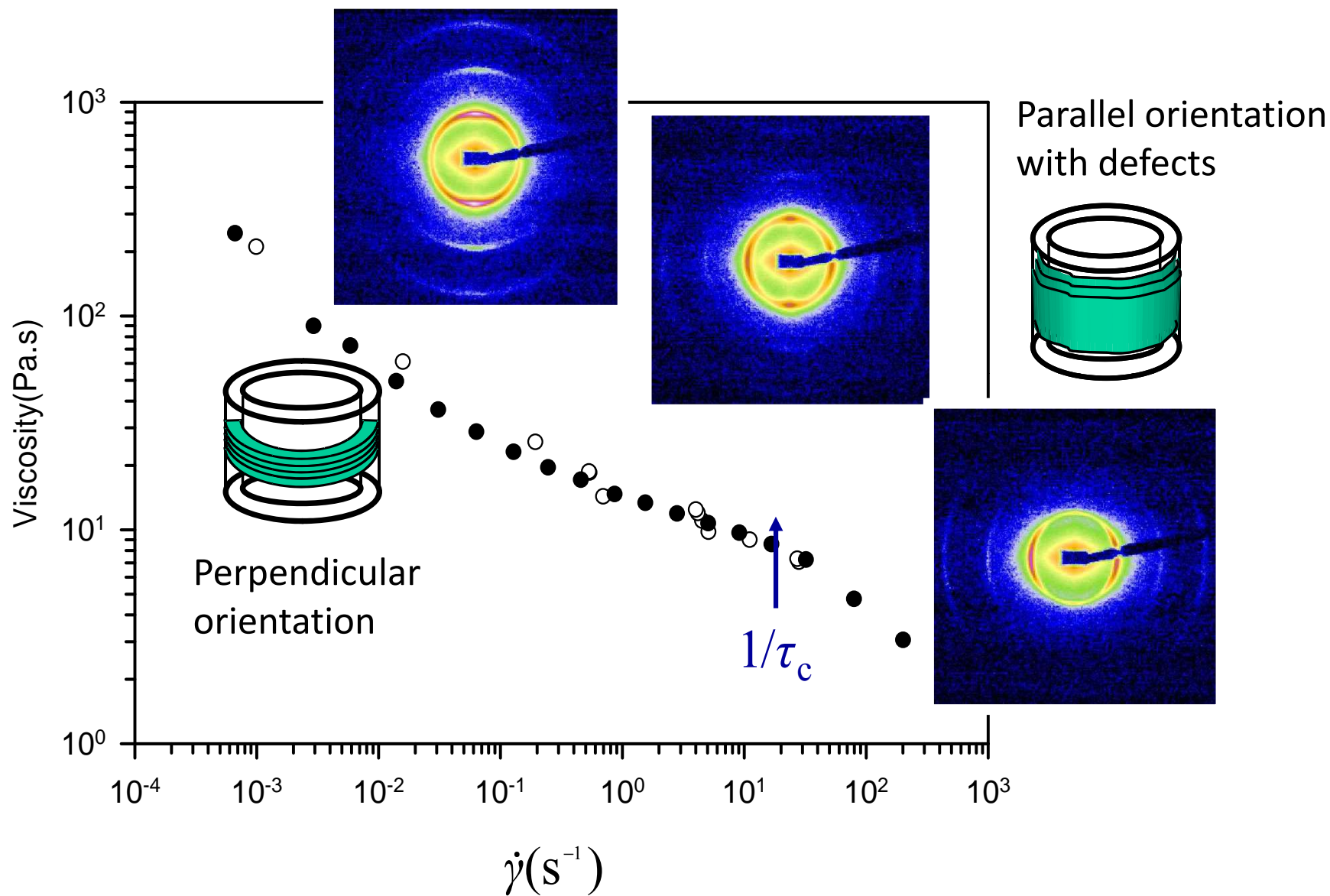
Transitions $\perp$ to $/\!/$ and $/\!/$ to $\perp$ proceed according to different mechanisms

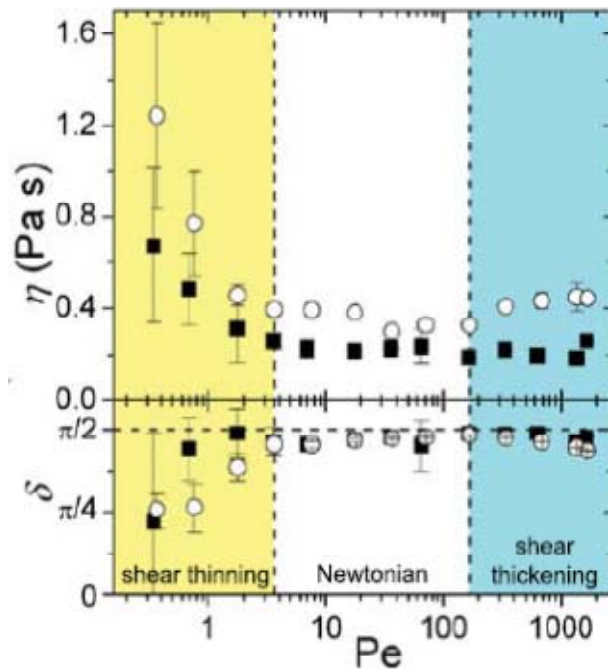# Rheo-confocal microscope
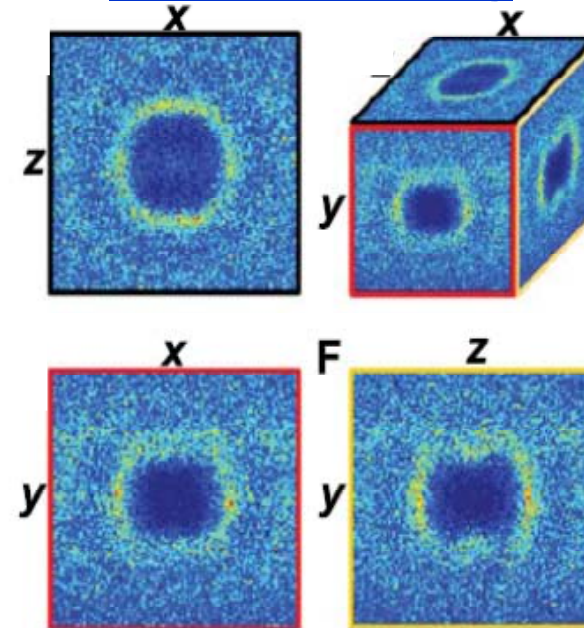
Principle of confocal microscopy

Implementation

L. Isa, R. Besseling, A. B Schofield, W. C. K. Poon, *Quantitative imaging of concentrated suspensions under flow*, Adv. Polym. Sci. **236**, 163 (2010)
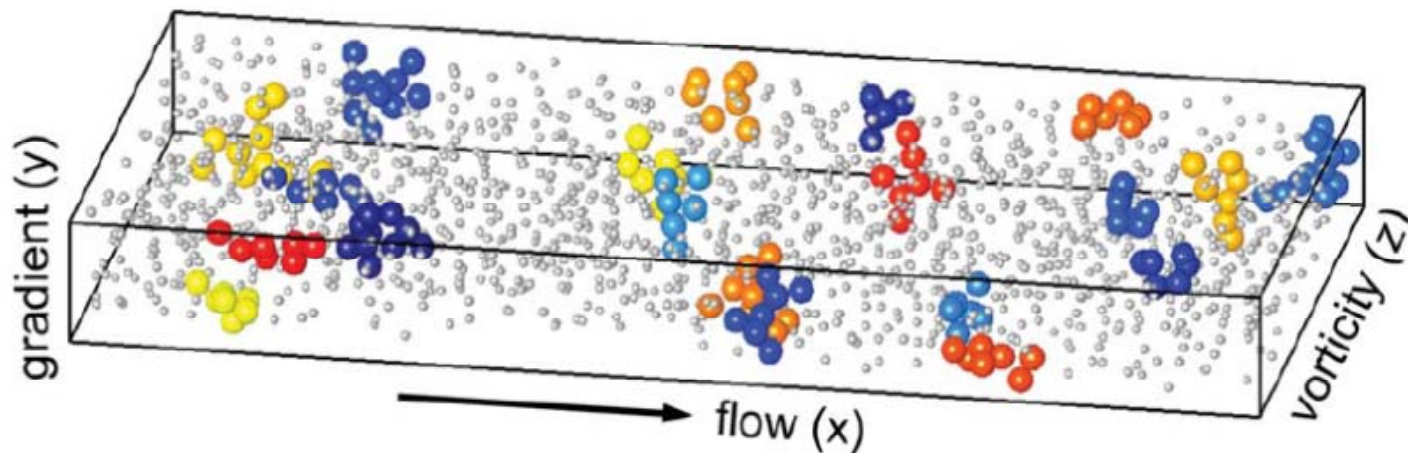
3D imaging of hard sphere suspensions in LAOS

Shear thinning

$\Phi = 0.34$
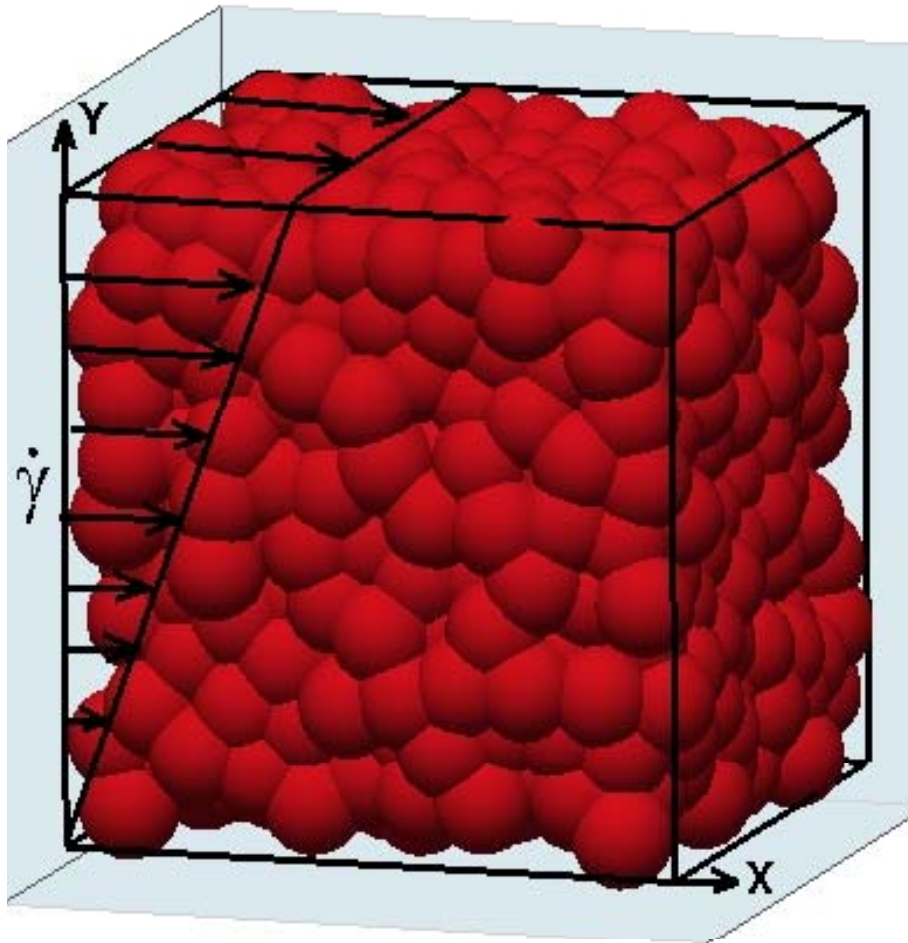Pe = 0.036

Shear thickening

$\Phi = 0.47$

53   X. Cheng, J.H. McCoy, J.N. Israelachvili, and I. CohenScience **333**, 1276 (2011)
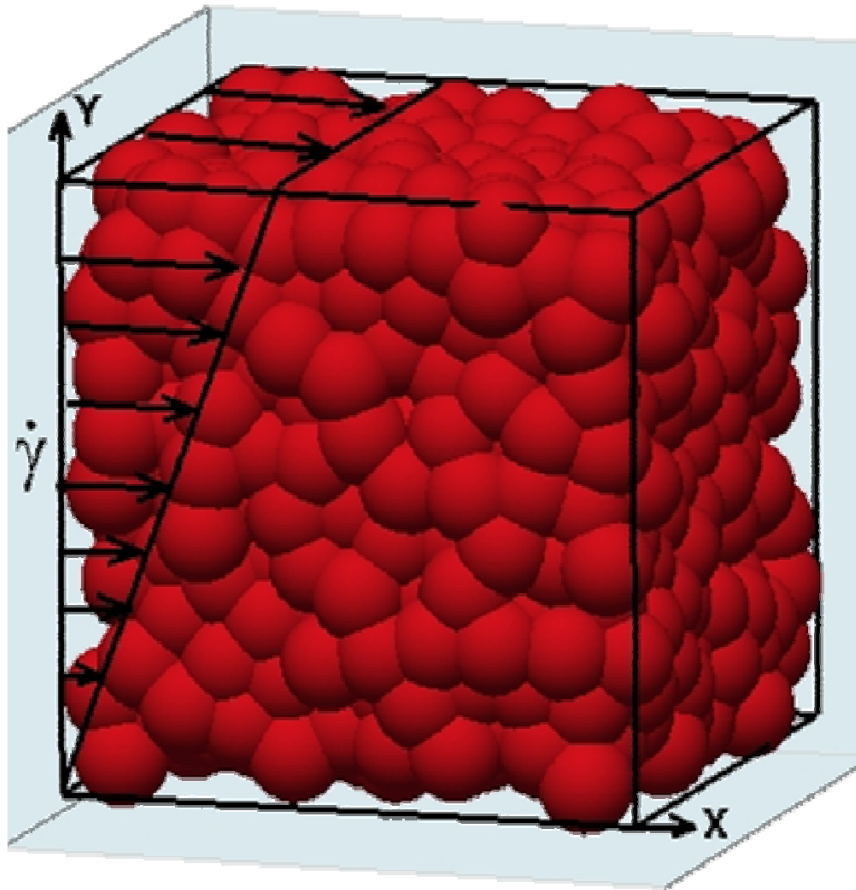
Computational rheology

Molecular-like dynamic simulations

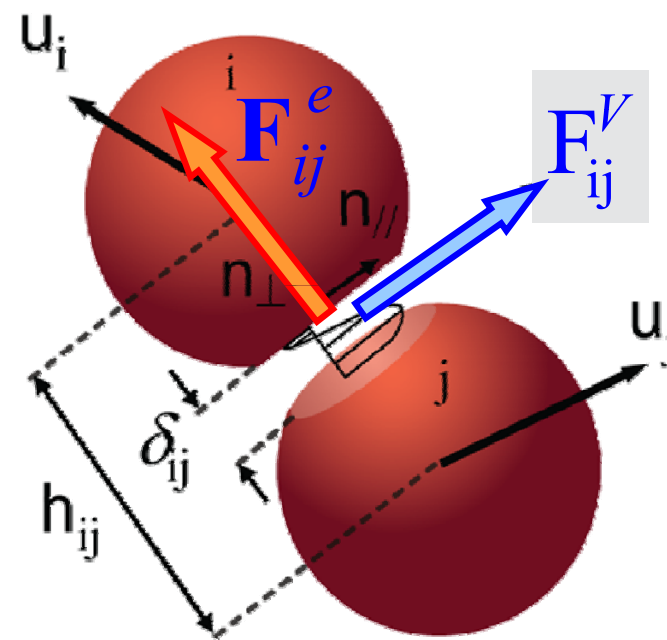Pairwise additive elastic interactions
Periodic boundaries
No inertia

Equation of motion:

$$\frac{d\vec{x}_i}{dt} = \vec{u}_i^\infty + \frac{f(\phi)}{6\pi\eta_s}\left[\sum_j \vec{F}_{ij}^e + \sum_j \vec{F}_{ij}^{EHD}\right]$$

Computational rheology of jammed suspensions

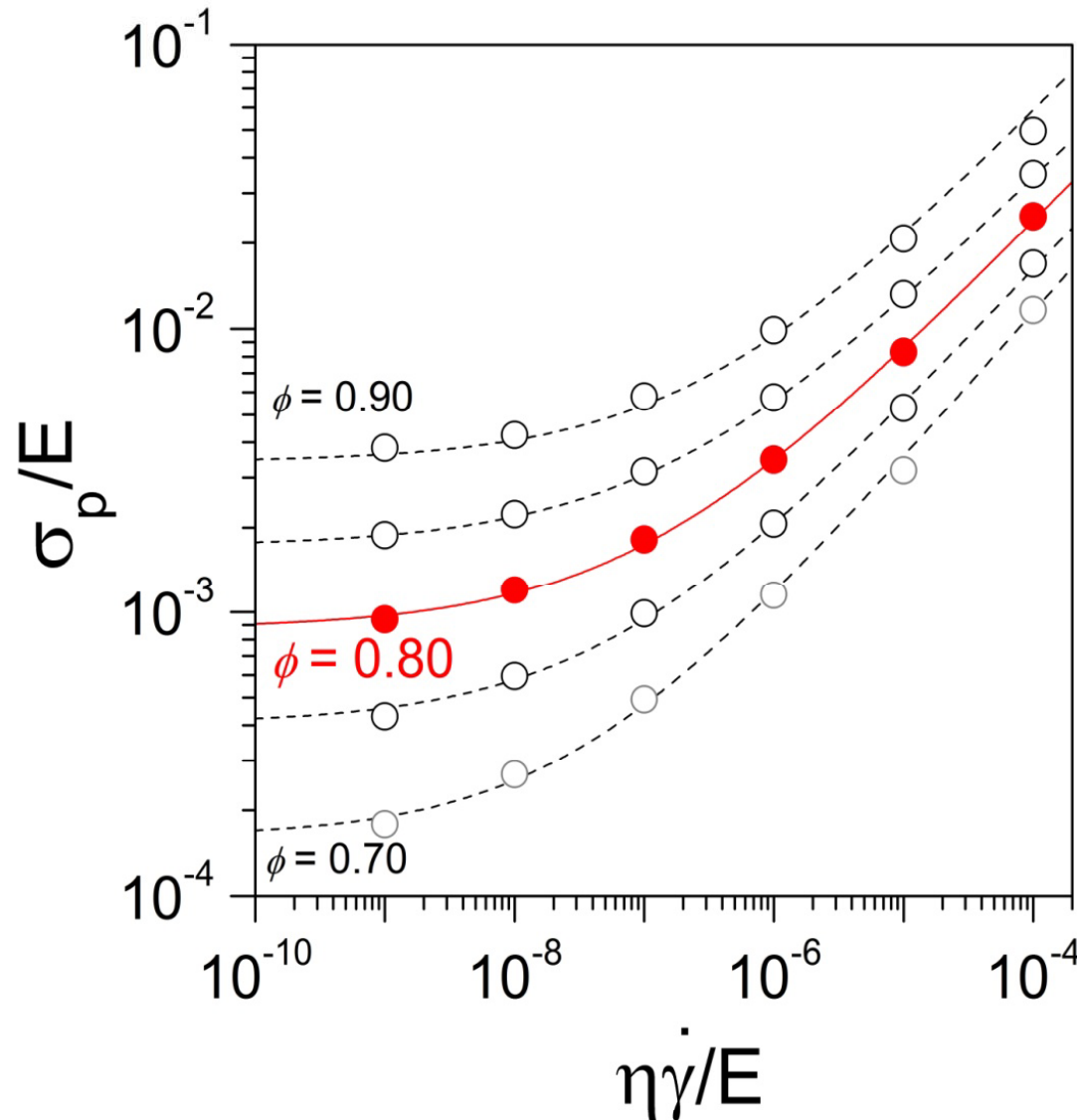Particles (modulus E) interact via normal elastic contact forces and sliding elasto-hydrodynamic lubrication forces

$$\frac{\eta_s \dot{\gamma}}{E^*}$$

$$\mathbf{u}_i = \frac{d\mathbf{x}_i}{dt} = \mathbf{u}_i^{\infty} + \frac{f(\phi)}{6\pi\eta_s}\left[\sum_j F_{ij}^e + \sum_j F_{ij}^V\right] \qquad \boldsymbol{\sigma} = -\frac{1}{V}\sum_{j}^{N}\sum_{i>j}^{N}(\mathbf{x}_i - \mathbf{x}_j)\left(F_{ij}^e + F_{ij}^V\right)$$
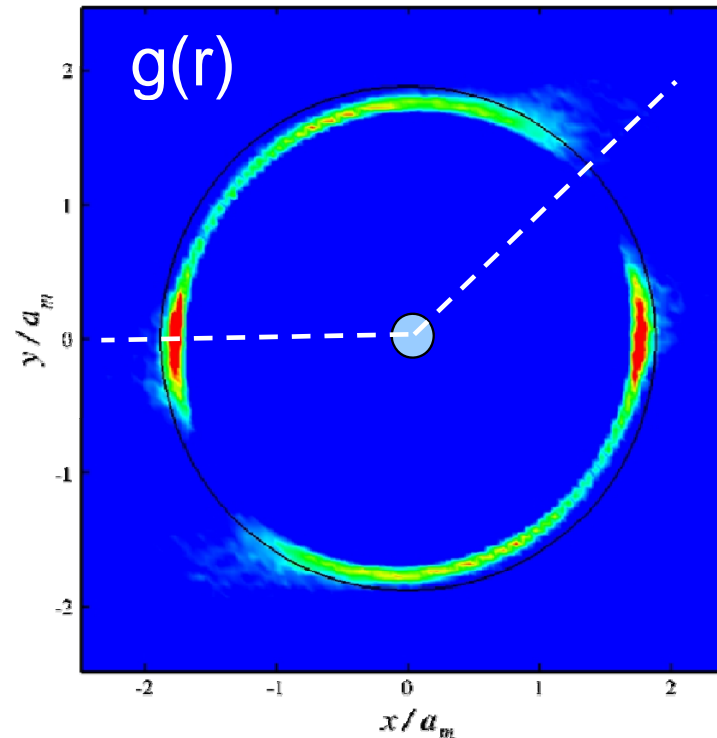
Flow curves
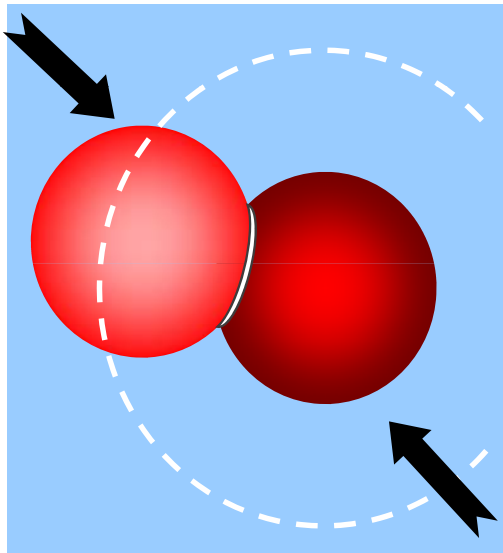

Yield stress behaviour
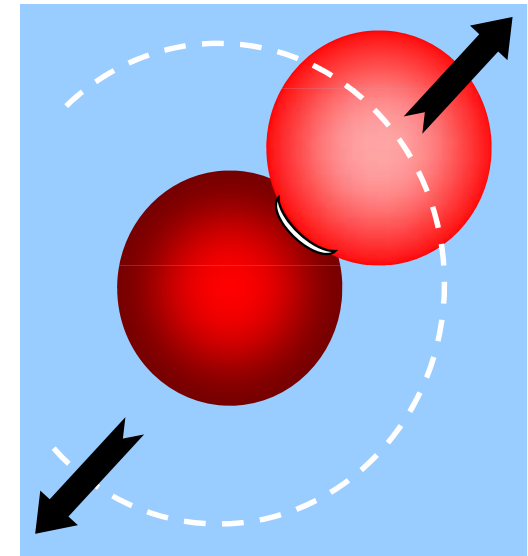(matches experiments)
Microscopic time scale: $\tau_0 = \eta/E$

$$\sigma_p = \sigma_y + k\left(\frac{\eta\dot{\gamma}}{E}\right)^{0.5}$$

Computation of pair correlation function

Compression: accumulation

Extension: depletion

g(r)

Flow causes a redistribution of contacts
(radial compression and angular asymmetry)
σ, N_1 and N_2 are calculated from g(r)

 J. Seth, L. Mohan, C. Locatelli,, M. Cloitre, R. T. Bonnecaze, Nature Materials **10**, 838 (2011)